Adsorptive Removal of Nickel from Aqueous Solution by Palm Seeds-based Magnetic Biochar

Kola A. Azalok

Submitted to the
Institute of Graduate Studies and Research
in partial fulfillment of the requirements for the degree of

Master of Science
in
Chemistry

Eastern Mediterranean University
January, 2017
Gazimağusa, North Cyprus

Approval of the Institute of Graduate Studies and Research

Prof. Dr. Mustafa Tümer
Director

I certify that this thesis satisfies the requirements as a thesis for the degree of Master of Science in Chemistry.

Assoc. Prof. Dr. Izzet Sakallı
Chair, Department of Chemistry

We certify that we have read this thesis and that in our opinion it is fully adequate in scope and quality as a thesis for degree of Master of Science in Chemistry.

Assoc. Prof. Dr. Mustafa Gazi
Supervisor

Examining Committee

1. Prof. Dr. Osman Yılmaz

2. Assoc. Prof. Dr. Mustafa Gazi

3. Asst. Prof. Dr. Akeem Oladipo

ABSTRACT

Here, the possibility of using biomass wastes such as palm seed as a suitable precursor for the preparation of magnetically responsive adsorbent was explored. Magnetic biochars (MB) were prepared from raw palm seed in the presence of iron oxide (Fe_3O_4) particles and utilized for adsorption of nickel. The thermal decomposition processes of the adsorbents were determined by thermogravimetric analysis. The physical structure and textural characteristics of the adsorbents were investigated. The effects of adsorption parameters, including pH, adsorbent dosage, temperature, interfering ions and contact time were investigated.

The results showed that the magnetic biochar exhibited high sorption capacity, excellent dispersion and convenient separation after spent. The relationship between the MB and the pollutant (Ni^{2+}) was established to follow Langmuir model, described well by pseudo-second-order kinetic and intraparticle diffusion played an important role in the sorption process. 27.8 mg/g was obtained as the maximum nickel uptake. The values of thermodynamic parameters revealed that the sorption process depended on the temperature of the medium, was spontaneous and endothermic in nature. Lastly, the magnetic biochar was regenerated via a simple technique and reuse with no significant loss in activity, suggesting that MB is technically and economically efficient.

Keywords: Magnetic biochar, palm seed powder; nickel (II) ions, adsorption

ÖZ

Burada, palmiye tohumlarından oluşan biyokütle atıkların, manyetik olarak duyarlı adsorban hazırlanmasında uygun bir ön madde olarak kullanılma olasılığı araştırılmıştır. Manyetik biyokömür (MB), demir oksit (Fe_3O_4) partiküllerinin varlığında işlenmemiş palmiye tohumlarından hazırlanmış ve nikelin adsorpsiyonu için kullanılmıştır. Adsorpsiyon maddelerinin ısıl bozunma prosesleri termogravimetrik analiz ile belirlenmiştir. Adsorbanların fiziksel yapısı ve dokusal özellikleri araştırılmıştır. Adsorpsiyon dozu, sıcaklık, karışan iyonlar ve temas süresi gibi adsorpsiyon parametrelerinin etkileri araştırılmıştır.

Sonuçlar manyetik biokömürün, yüksek sorplama kapasitesine, mükemmel dispersiyona ve uygulama sonrası kolay ayrılabilme özelliğine sahip olduğunu göstermektedir. MB ve kirletici (Ni^{2+}) arasındaki ilişki yalancı-ikinci dereceden kinetik ve intrapartikül difüzyonun sorpsiyon sürecinde önemli bir rol oynadığı Langmuir modelini izleğini göstermiştir. Maksimum nikel tutumu 27.8 mg/g olarak belirlendi. Termodinamik parametrelerin değerleri, sorpsiyon işleminin ortam sıcaklığına bağlı olarak, kendiliğinden ve endotermik olduğunu ortaya koymuştur. Son olarak, manyetik biokömürün basit bir teknikle rejenere edilmesi ve etkinliğinde önemli bir kayıp olmaksızın yeniden kullanımı, MB'nin teknik ve ekonomik açıdan verimli olduğunu düşündürmektedir.

Anahtar Kelimeler: Manyetik biokömür, palmiye tohum tozu; Nikel (II) iyonları, adsorpsiyon

DEDICATION

I would like to dedicate my thesis to my primary family. My dear dad, Mr. Abedalmulaleb Ahmed Azalok and precious mum, Mrs. Kyriyha Mohammed Mahfouth. Thank you both for encouraging and giving me strength to reach my educational goals. To my sisters, brothers, aunts, uncles, and all my relatives, I say big thank you, God protect and bless you for all your spiritual and financial supports. Many thanks to my compassionate husband, Mr. Ali Nasseralden Azalok for his constant support and encouragement. To my darling daughter, Aleen Ali Azalok, may you live long under Allah's protection.

ACKNOWLEDGMENT

First of all, I am grateful to Almighty **Allah** for giving me ability and strength to achieve my goals and complete this manuscript.

To my supervisor, Assoc. Prof. Dr. Mustafa Gazi, who helped me to choose this topic, God bless you and reward you in many folds. Thanks for providing me all the needed information and necessary facilities to complete the thesis.

I am simply overwhelmed with gratitude and appreciation to Asst. Prof. Dr. Akeem Oladipo, who contributed immensely to the success of this work. May Allah bless you abundantly sir for the invaluable guidance and encouragement. I do appreciate your time and effort in checking this thesis word by word.

I acknowledge my best girl-friend, Zainab Ojoro for her constant help and guidance during my studies at EMU. I would also use this opportunity to thank you to Wihad Khaleal, Ayo, Adamo, Mammon and all other colleagues at the Eastern Mediterranean University. My utmost appreciation to our landlord and landlady, Mr. Emirali and Mrs. Gulay Sari…I can say you guys are all the best people I have met in Cyprus. God bless you all!

Lastly, I will record my sense of gratitude to all whom, directly or indirectly have lent their helping hand in this thesis.

TABLE OF CONTACT

LIST OF TABLES

LIST OF FIGURES

LIST OF ABBREVIATIONS

AB	Alginate-based composite beads
BC	Biochar
CS-MAA	Chitosan methacrylic acid nanoparticles
CTS-g-AP	Chitosan-graft-polyacrylamide
DTA	Differential thermal analysis
DTG	Differential thermogravimeter
Fe_3O_4	Iron nanoparticles
HM	Heavy metals
HTC	Hydrothermal carbonization
MB	Magnetic biochar
MCL	Maximum contamination limit standards of heavy metals
MN	Magnetic material
MPSP	Magnetic palm seed powder
n-HApAg	Nano-hydroxyapatite/alginate composite beads
PFO	Pseudo first order
PS	Palm seeds (feedstock)
PSO	Pseudo second order
PSP	Palm seeds powder
RM	Red mud
TGA	Thermogravimeter analysis

Chapter 1

INTRODUCTION

1.1 Background of study

Boom in industrialization globally has led to monumental use of heavy metals, resulting in increased flow of metal-based substances in the aquatic environment. Recently, the World Health Organization (WHO) has warned that the carcinogenic threat to living organisms posed by exposure to heavy metals is deadly. These residual metals in the environment have adverse effects on aquatic ecosystems (Barakat, 2010), attributed to their persistence and recalcitrant nature, toxicity, and aggregation in the living organisms (Qin et al., 2012).

Among these metals, nickel is one of the most used in the manufacturing process of batteries, coins, super alloys, stainless steel, and sintered metal coatings,etc (Shrestha et al., 2014). Based on animal and human studies, nickel carbonyl is ascertained as the most severely toxic nickel compound, causing devastating damage to the respiratory system in humans and animals (Oladipo and Gazi, 2015). Hence, the removal of nickel from aqueous medium is extremely necessary (Qin et al., 2012).

Several efforts and methods have been proposed for nickel ion removal from aqueous solutions. Adsorption, a simple and cost-effective method of environmental waste control has been established to be a substitute to time-consuming traditional technologies (ion exchange, chemical precipitation, reverse osmosis and evaporative

recovery). Despite the performance and success of these traditional techniques, they have varying disadvantages limiting their wider industrial applications (El-Sadaawy and Abdelwahab, 2014).

Various materials have been utilized as adsorbents ranging from inorganic nanoparticles to biomaterials. But recently, concerted efforts have been directed towards the use of biomaterials. Bio-based materials are unused environmentally friendly resources, available in large quantities and have the potential to be utilized as economic adsorbents (Barakat, 2010; Oladipo and Gazi, 2014). Due to the persistence and bioaccumulation nature of nickel-based pollutants, intense attention has been directed towards high performance, low cost and efficient adsorbent that can be employed to eliminate nickel from aqueous solution.

Inspiring results have been recorded so far. However, a study on waste palm seeds as an adsorbent or precursor for fabrication of high-performance magnetic biochar is less. Hence, there is a need to investigate the adsorptive ability of biochar obtained from palm seeds. Thus, this study focussed on the utilization of palm seed-based magnetic biochar for the removal of nickel from simulated aqueous solution.

1.2 Research questions

Important questions to be answered in this study are:

a. Can waste palm seeds be converted to high magnetically responsive adsorbents?
b. Can the magnetic biochar outperform reported adsorbents for nickel removal
c. How can adsorption parameters be modified to obtain maximum nickel removal?

d. Can the spent magnetic biochar be regenerated and reuse to make the process of nickel removal more economical?
e. How stable is the fabricated magnetic biochar towards chemical and thermal degradation?

1.3 Research objectives

The specific goals of this study are:

a. To access the potential of palm seed-based magnetic biochar to remove nickel from simulated aqueous solutions.
b. To investigate the effects of various sorption parameters such as adsorbent dosage, pH, interfering ions, temperature and treatment time in the removal of nickel.
c. To study the sorption mechanism, kinetics and obtain thermodynamic information specific to the magnetic biochar during the nickel removal.
d. To quantify levels of nickel adsorbed under laboratory conditions.
e. To investigate the potential recovery of nickel from adsorbent-loaded nickel.

1.4 Limitation of the study

The current study focused on the utilization of fabricated magnetic biochar for removal of nickel via batch system under laboratory conditions. The efficiency of the as-prepared adsorbent under industrial conditions (continuous system) was not investigated. Similarly, the performance of the adsorbent in the presence of real wastewater rich in nickel was not checked. Thus, the above-mentioned points limit this research.

1.5 Outlines of research

The following outline was strictly considered during the preparation of this thesis as depicted in Fig.1 below:

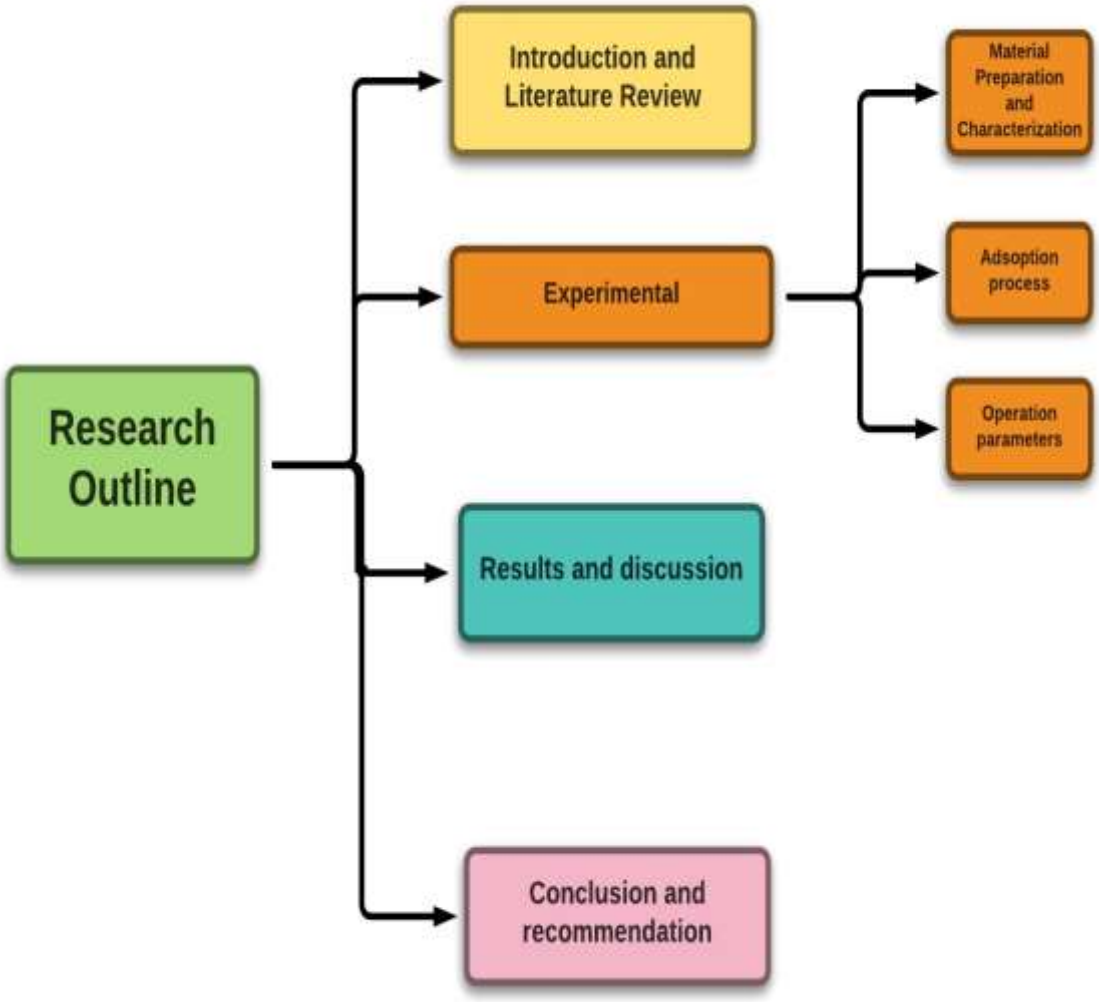

Figure 1: Thesis outline

Chapter 2

LITERATURE REVIEW

In the recent past, many researches have been devoted to investigating the application of biochar as an adsorbent for the elimination of effluents from aqueous solution. This concerted attention is because; biochar is cheap, the precursors are easily available, and it exhibits a high-efficiency for the removal of pollutants from the domestic and industrial wastewaters (Barton et al., 2015; Tan et al., 2015). Various efforts have been directed towards the use of cheaply available resources such as palm seeds, vegetable wastes, coffee grounds, and all forms of agricultural wastes to produce biochars.

2.1 Heavy metals

Heavy metals including Hg, Pb, Zn, Ni, As, Cd, and Cu are the most common pollutants found in the aquatic environments, because of their non-biodegradability, carcinogenicity, and toxicity above certain thresholds (Inyang et al., 2015; Regina et al., 2015). Significant exposure to lead, cadmium, mercury, and arsenic poses severe threats to human health and all other living organisms (Barton et al., 2015). The main sources of heavy metal contamination to water streams is industrial activities, such as batteries manufacturing, metal plating, mining operations, and tanneries (Bailey et al., 1998).

The maximum contamination limits (MCL) of selected heavy metals are shown in Table 1. It is obvious from the table that, nickel is a priority pollutant due to its toxic

nature even at a lower concentration. That explains the reason for the wider investigation of nickel removal from industrial wastewater before discharged.

Table 1: The MCL standards for selected heavy metals (Barakat, 2010)

HM	Toxicities	MCL(ppm)
Cd	Human carcinogen, kidney hazardous, renal disorder	0.01
Zn	Nervous, thirst, depression, lethargy	0.80
As	Cancer, skin occurrence, vascular disease	0.050
Ni	Dermatitis, nausea, chronic asthma, human carcinogen	0.20
Cr	Vomiting, diarrhea, headache	0.05
Pb	Kidneys diseases, damage fertile mind, circulatory system	0.006
Hg	Rheumatism, neurological, kidney damage	0.00003

Various techniques have been applied for treatment of industrial wastewater rich in heavy metals. These methods include coagulation, ion exchange, floatation, chemical precipitation, electrode dialysis, membrane filtration, and adsorption (Regina et al., 2015). However, most of these methods have some disadvantages like high operation cost, low desorption rate and complex operation conditions. Therefore, there is a need to develop low-cost and easy technologies for remediation of pollutants (Inyang et al., 2015).

Among these techniques, adsorption has been widely applied and established as cost-effective, easy and efficient method for treatment of heavy metal laden wastewaters (Oladipo et al., 2015; Oladipo and Gazi, 2016; Regina et al., 2015). Recently, attention has been focussed on biochar as economic adsorbent for treating Inyang et

al. (2015) reported that copper and zinc were efficiently removed from contaminated water using biochar prepared from wood. Similarly, biochars prepared from soybean stalk have been reported to adsorb mercury from aqueous solution and the percentage removal reached 75-87% (Inyang et al., 2015). Hence, based on its economic, adsorptive potentials and environmental friendliness, biochar could be an alternative material for remediation of heavy metals. As shown in Fig.2, biochar has been applied in various facets.

Figure 2: Various applications of biochar **(**Tan et al., 2015)

2.1.1 Nickel, occurrence, and uses

Nickel is a silvery-white, hard, malleable and ductile metal. It has an atomic number of 28 and with electronic configuration of $1s^2$ $2s^2$ $2p^6$ $3s^2$ $3p^6$ $3d^8$ $4s^2$. It has widespread distribution in the environment (in water, air, and soil) (Regina et al.,

2015), and the natural sources of atmospheric nickel include dust from volcanic emissions and the weathering of rocks (Duda-Chodak and Blaszczyk, 2008).

Nickel is the 24th most abundant element in the Earth's crust, comprising about 3% of the composition of the earth. It is the 5th most abundant element by weight after iron, oxygen, magnesium and silicon. It is a member of the transition series and belongs to group 10 on the periodic table along with Fe^{2+}, Co^{2+}, Pd^{2+}, Pt^{2+} and five other elements. The 2+ valence of nickel is its prevalent oxidation state under environmental conditions, and other valences (-1, +1, +3, and +4) are less frequent (Cempel and Nikel, 2005).

Nickel and nickel compounds have many industrial and commercial applications. Most nickel is used for the production of stainless steel, metallurgical and other nickel alloys with high corrosion and temperature resistance (Cempel and Nikel, 2005). Electroless nickel coatings possess splendid tribological properties such as high hardness; good wear resistance, and corrosion resistance. For this reason, electroless nickel has found wide applications in aerospace, automobile, electrical and chemical industries (Sahoo and Das, 2010).

The maximum contamination limit (MCL) standard of Ni^{2+} ion is 0.2 mg/L. However, the acceptable limit of Ni^{2+} ion in drinking water is 0.01 mg/L and the industrial discharge limit in wastewater is 2 mg/L. Therefore, wastewaters containing nickel are required to be treated before discharge into the environments (Olad et al., 2013).

2.1.2 Effects of nickel on the environment

Increasing uses of nickel-containing products results into the continuous release of nickel into the environment at all levels. This poses an adverse risk to plants and animal health (Duda-Chodak and Blaszczyk, 2008). Pollution of soil by nickel is not new; this has been reported to cause different physiological alterations and diverse toxicity symptoms like necrosis and chlorosis in various plant species (Asati et al., 2016).

2.1.3 Nickel effects on human health

People are exposed to nickel through drinking polluted water, inhalation, eating food or smoking cigarettes. In small doses nickel is essential, but exposure to high level of nickel can be hazardous to human health. Epidemiological study on workers of electroplating factory indicated that workers exposed to nickel compounds showed a high risk of nasal, larynx, prostate and lung cancers (Nagajyoti et al., 2010).

2.2 Remediation technology: Adsorption

Adsorption is the adhesion of ions, atoms, or molecules from an adsorbate to a surface. A basic concept of adsorption process involves the adsorbent being in contact with the bulk phase and the interfacial layer (Gupta et al., 2009). The material in the adsorbed state is called the '*adsorbate*,' while that in the bulk phase before being adsorbed is referred to as '*adsorptive*.' The term '*sorption*' denotes both absorption and adsorption when both cannot be distinguished or take place simultaneously (Dabrowski, 2001).

2.2.1 Factors affecting adsorption

The removal of pollutants such as heavy metals, dyes and life-threatening toxic substances from aqueous systems tends to be influenced by many factors such as

temperature, contact time, solution pH, the integrity of the adsorbents and initial concentration of the pollutants just to mention a few.

2.2.1.1 Properties of adsorbent

The source of adsorbents, feedstock materials, preparation conditions, and modification methods can have controlling effects on the adsorptive characters of the adsorbents. Chen et al. (2012) reported that the pyrolysis temperature of a biochar affects the average removal percentage of pollutants, insisted that heat affect the degree of carbonization of biochar. Highly pyrolytic materials possess enhanced adsorption capacity towards target pollutants. Xu et al., (2011) examined the uptake of methyl violet by biochars obtained from four residual crops. The researchers pointed that the source of materials for preparation of biochar had influencing effects on the uptake capacities of the biochars. The uptake capacities in their study followed the following order: canola straw char > peanut straw char > soybean straw char > rice hull char. They concluded that uptake capacity was influenced by the number of active negative charges on the biochar surface.

2.2.1.2 Solution pH

The pH of the solution is one of the most significant variables affecting adsorption process. The surface functional groups on the adsorbents get protonated or deprotonated with increasing or decreasing the solution pH. According to the pH point zero charge (pH_{pzc}), the surface of the adsorbent becomes positively charged when the pH of the solution is less than the pH_{pzc}, resulting in competition between the active sites on the adsorbent and cationic pollutants. Hence, low adsorption capacity will be recorded (Ghasemi et al., 2014). However, the adsorbent surface becomes negatively charged when the solution pH is greater than the pH_{pzc}, thus,

attractive interaction between negatively charged adsorbent and cationic pollutants occur (Oladipo et al., 2015).

2.2.1.3 Coexisting or interfering ions

The co-existence of ions in aquatic environment exerts significant influence on the equilibrium adsorption capacity. However, precise mechanism behind these influences remains equivocal, because some studies reported increased adsorption capacity in the presence of some interfering ions while others reported a decreasing trend. According to the review article by (Tan et al., 2015), they reported that some authors found the adsorption of polychlorinated biphenyls on biochar increased when metal cations and humic acid were present in the medium. While other researchers reported that phenanthrene adsorption decreased in the presence of mercury (II) ions in the aqueous solution.

2.2.1.4 Adsorbent dosage

The percentage removal and uptake capacity are largely affected by dosage of adsorbents. The amount of crystal violet (CV^+) adsorbed decreased from 580.2 to 30.6 mg/g with increasing adsorbent (acid-activated bentonite clay) dosage from 10 to 100 mg. Meanwhile, the CV^+ removal percentage increased from 40.4 to 96.0% as reported by Oladipo and Gazi (2014). They attributed the increases in percentage removal to increased adsorbent surface area and availability of more active sorption sites. Similarly, Kooh et al. (2016), investigated the effect of the adsorbent dosage on the removal of methyl violet dye, they reported rapid increases in percentage removal when the adsorbent quantity increased (0.01 to 0.04 g).

2.2.2 Adsorption isotherms

Adsorption isotherm models are commonly used to illustrate the interactive relationship between adsorbate and adsorbent. The commonly applied isotherms

include Langmuir, Freundlich, Redlich-Peterson, Temkin, and Dubinin–Raduskevich (D–R) as described in Table 2 (Inyang et al., 2015):

Table 2: General isotherm models for adsorption process

Model types	**Equation**	**Description**	**Reference**
Freundlich (Heterogeneous adsorption)	$q_e = k_F C_e^{1/n}$ (1)	q_e is equilibrium uptake capacity; n is a constant indicative of sorption intensity.	Wang and Chen, 2009
Langmuir (Homogeneous adsorption)	$q_e = \frac{q_{\max} b C_e}{1 + b C_e}$ (2)	q_e is an equilibrium sorption capacity, C_e is the equilibrium concentration of solute in solution, q_{max} and b are Langmuir constant rated to maximum- sorption capacity	Shrestha et al., 2014
Redlich-Peterson (Heterogeneous & homogeneous adsorption)	$q_e = \frac{k_{RP} \times C_e}{1 + \alpha_{RP} + C_e^{\beta}}$ (3)	k_{RP}, α_{RP}, and β are the R-P parameters. The exponent β lies between 0–1.	Wang and Chen. (2009)
Temkin	$q_e = \frac{RT}{b} \ln K_T C_e$ (4)	R is the universal gas constant (8.314 J/mol k), T is the absolute temperature. A (L/mg) is the maximum binding energy, and B is the heat of adsorption (kJ/mol)	Wang and Chen. (2009)
Dubinin–Radushkevich	$\ln q_e = \ln q_m - k\varepsilon^2$ (5)	ε is Polanyi potential and k is free (mean) energy of sorption.	Matouq et al., 2015

2.2.3 Adsorption kinetics

Various mathematical models have been applied to describe the sorption kinetics of pollutants on various adsorbents. These kinetic models have been classified into two main types: reaction–based and diffusion based models (Ho et al., 2000). Elovich pseudo-second-order, intraparticle diffusion and pseudo-first-order models are

common models applied to investigate adsorption rate. The corresponding equations of each kinetic model are described according to Eqs. 6–9:

Pseudo first order, $\ln (q_e - q_t) = \ln q_e - k_1 \, t$ (6)

Pseudo-second order, $q_e = \frac{k_2 q^2_e t}{1 + k_2 q_e t}$ (7)

Elovich, $q_e = \frac{1}{\beta} \ln(\alpha \beta t + 1)$ (8)

Intraparticle diffusion, $q_t = k t^{1/2} + C$ (9)

Where q_e and q_t are the amount of metal adsorbed at equilibrium and time t per unit mg/g, respectively. k_1 (1/min) and k_2(1/min) are the first and second-order rate constants, respectively.The α (mg/g min) and β (g/mg) are the initial Elovich sorption and desorption rate constant at time t, respectively, k is the intraparticle diffusion rate constant (mg/gmin$^{-0.5}$), and C is a constant (Inyang et al. 2015).

Chapter 3

EXPERIMENTAL

3.1 Materials and equipment

Analytical grade reagents were used. Palm seeds were obtained within the Eastern Mediterranean University campus. Reagent grade of nickel nitrate hexahydrate, sodium hydroxide, ferrous and ferric sulfate, hydrochloric acid, H_2SO_4 were purchased from Sigma-Aldrich. The laboratory pH meter (HANNA, model; HI 98127) was employed to determine the pH of solutions. A conventional oven (BINDER GmbH, Model BD115-EZ) was used for drying the raw materials. A muffle furnace (Nabertherm GmbH model) was used for calcination of the samples. The concentration of nickel left in solution was analyzed by UV–vis spectrometer (Beijing, Version 5.0, T80+). The thermogravimetric data of the prepared adsorbents were obtained using TGA– DTA machine from HITACH (STA7300).

3.2 Preparation of adsorbent

3.2.1 Pre-treatment of palm seeds (feedstock)

The raw material gathered were isolated and husked to get the clean seeds. These seeds were washed several times with distilled water and soaked for a night in a beaker containing distilled water to removal any impurities (as is shown in Fig.3). The washed samples were then dried in the conventional oven at 80˚C for 48 hours. The dried samples were ground using a blender into a powdered form and sieved to the desired size.

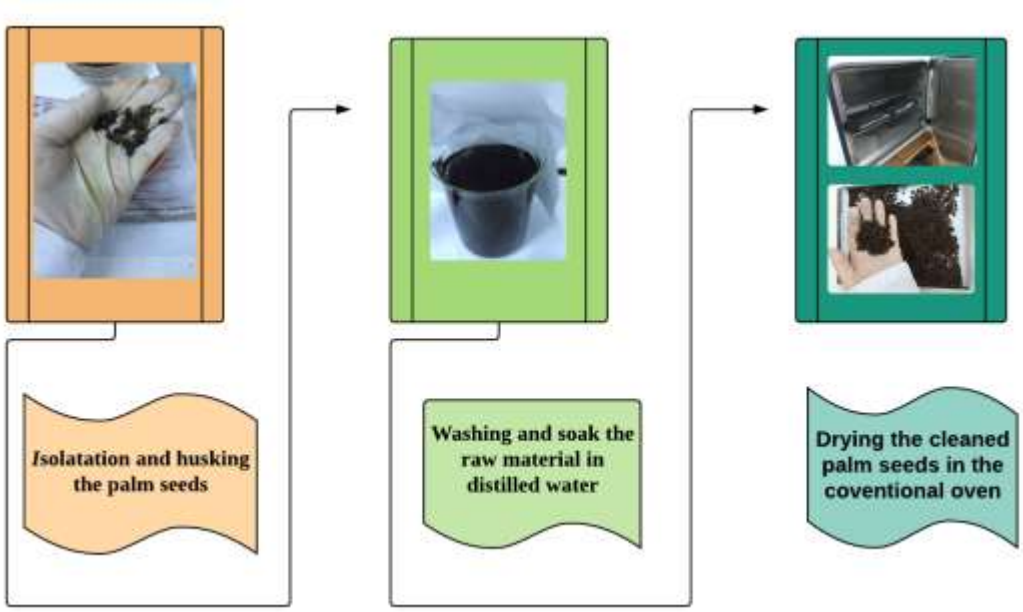

Figure 3: Pre-treatment of feedstock steps (taken by Kola)

3.2.2 Preparation of magnetic material (MN)

Fe_3O_4 nanoparticles were prepared by dissolving 12.0g of $FeSO_4$ with 6.0g of $Fe_2(SO_4)_3$ in 200ml distilled water. Then, 120mL of NaOH (6.0M) was added slowly to the solution at 30 ºC and continuously stirred (200rpm) for 1 h. The black precipitate obtained was filtered using a vacuum filtration (as in Fig.4), washed many times using deionized water and dried (80 ºC) for 24 h.

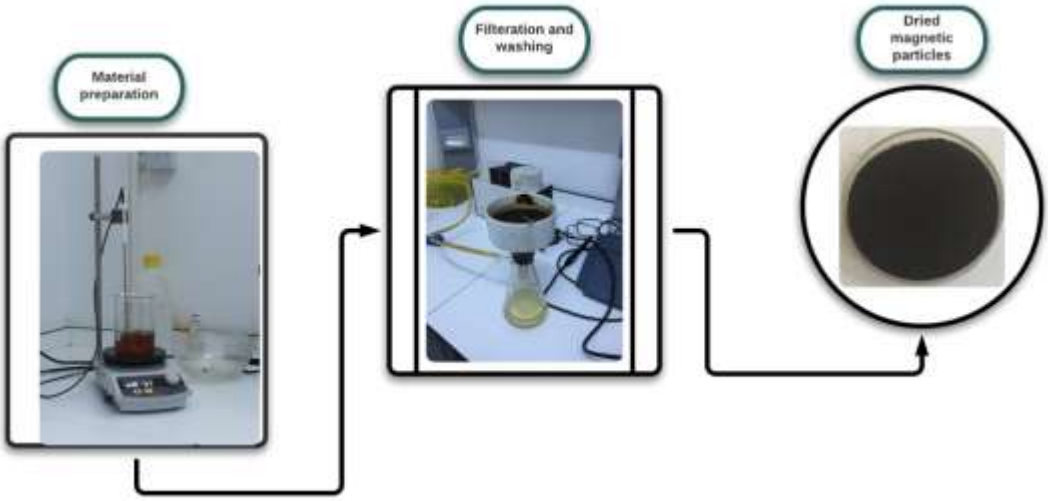

Figure 4: Pictorial representation of Fe_3O_4 nanoparticles preparation (taken by Kola)

3.1 Preparation of magnetic palm seed powder (MPSP)

For the preparation of magnetic palm seed powder (MPSP), 20g of dried palm seed powder were added to a mixture of freshly prepared ferric and ferrous solutions under constant stirring. 60 mL of NaOH (3.0 M) was introduced slowly to the mixture and stirred continuously at 30 ºC for 1 h. The brownish black precipitate filtered by a vacuum filtration, washed thoroughly with distilled water and dried at 80 ºC for 24 h. Various ratios were prepared accordingly as shown in Figure 5.

Figure 5: Various ratios of MPSP (taken by Kola)

3.2.4 Preparation of magnetic biochar (MBC)

After preparation of the precursors, 6.0g of dried MPSP was calcined in a muffle furnace at 400 ºC for 1 h, at 600 ºC for 1h, and at 600 ºC for 2 h to produce various types of MBC, ground to fine powder and stored until use, as shown in Fig 6.

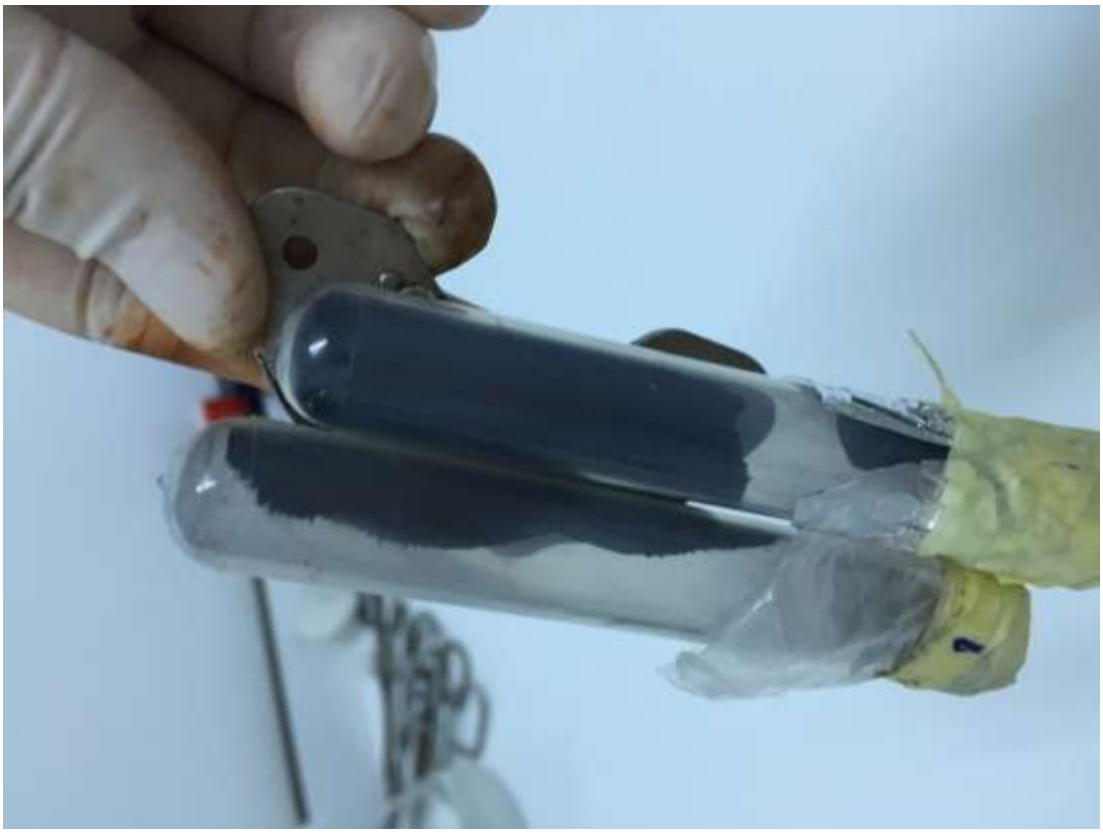

Figure 6: Magnetic biochar derived from palm seeds (adsorbent) (taken by Kola)

3.3 Adsorbate preparation

A stock solution of nickel (1000 mg/L) was prepared by dissolving 4.95 g of nickel nitrate hexahydrate [Ni $(NO_3)_2.6H_2O$] in 1L of deionized water. Working solutions were prepared via serial dilutions of the stock. Obtained calibration curve presented in Fig.7.

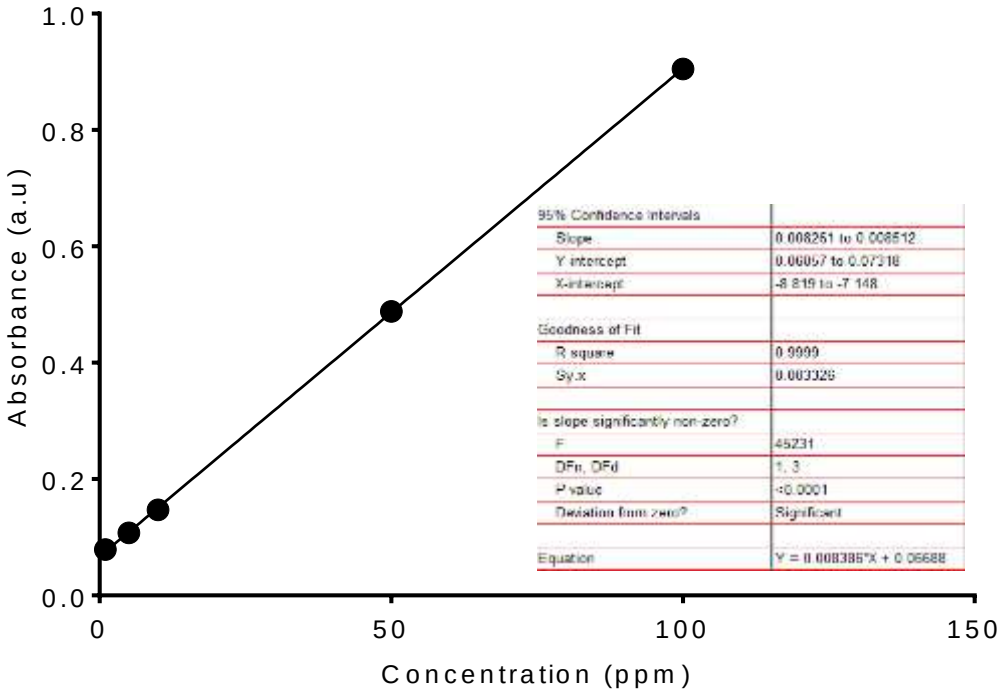

Figure 7: Calibration curve for nickel

3.4 Batch experiments

Here, the adsorptive potential of the prepared adsorbent was evaluated via a batch system. The effect of pH on nickel (II) adsorption was examined by agitating 0.5g of adsorbent in 25 mL of nickel solution (200mg/L) at different pH values (3–10). The effect of adsorbent dose (0.25–1.0 g), and the contact time (20–720 min) were investigated at 200 rpm. The effect of initial nickel concentration and the equilibrium studies were carried out by adding 0.5 g of MB with 25mL of nickel solutions (1–200mg/L) at 25˚C ± 1. Periodically, the magnetic biochar was separated by external magnet from the bulk phase and the residual nickel concentration analyzed at 232 nm. The nickel uptake capacity (q_e) and removal efficiency (R%) were obtained using Eqs. 5 and 6, respectively (Ghasemi et al. 2014):

$$q_e = \left[\frac{C_0 - C_e}{m_{MB}} \right] \times V \qquad (10)$$

$$R\,\%_{Ni^{2+}} = \left[\frac{C_0 - C_e}{C_0}\right] \times 100 \qquad (11)$$

Where C_o and C_e are the initial and equilibrium nickel concentration (ppm), respectively, m_{MB} refers to the amount of the adsorbent used, and V is the volume of adsorbate solution. Each experiment was performed in duplicate, and the average results reported.

3.5 Characterization of adsorbent

The specific surface area of the adsorbents was determined via the N_2 adsorption-desorption isotherms at 77K using Brunauer-Emmet-Teller equation. The pH point zero charge (pH_{pzc}) of the adsorbents was investigated. Briefly, 0.1M of sodium chloride solution was prepared, and the pH of the solution was adjusted ranges (1–10) using by adding 0.1M NaOH or HCl. Then, 0.2g of each sample were added into the pH adjusted NaCl solution, and agitated for 12h. The final pH was estimated by using a pH meter, and the pH_{pzc} was determined.

The physicochemical parameters of the samples such as percentage yield, weight loss, bulk density, ash content, moisture content, magnetic saturation, coercivity (O_e), and pH value were determined. The thermogravimetric and differential thermal analyses (TGA–DTA) of the samples were obtained. The heating process started at 50 ˚C, and then increased to 800˚C with a temperature rate change of 10˚C per minute under N_2 atmosphere (20ml/min).

Chapter 4

RESULTS AND DISCUSSIONS

4.1 Characterization

The specific surface area of the adsorbents was determined as 0, 123.8, and 135 m^2/g for PSP, MN, and MB, respectively. The pH point zero charge of the samples is shown in Fig. 8 and results of the physicochemical analyses are tabulated (Table 3).

Table 3: Physicochemical analysis of PSP, MN, and MB

Parameters	**Values**		
	PSP	**MN**	**MB**
Yield (%)	61	29.87	50.42
Weight loss (%)	39	70.13	49.58
Bulk density (gmL^{-1})	0.5071	0.591	0.754
Ash content (%)	2.73	0	0
Moisture content (%)	0.6	0.9	0
pH_{pzc}	6.3	7.0	2, 5
Saturation magnetization(emu/g)	0	88.9	65.8
pH value	6.5	7.3	4.6
Coercivity (O_e)	0	123.8	135.8

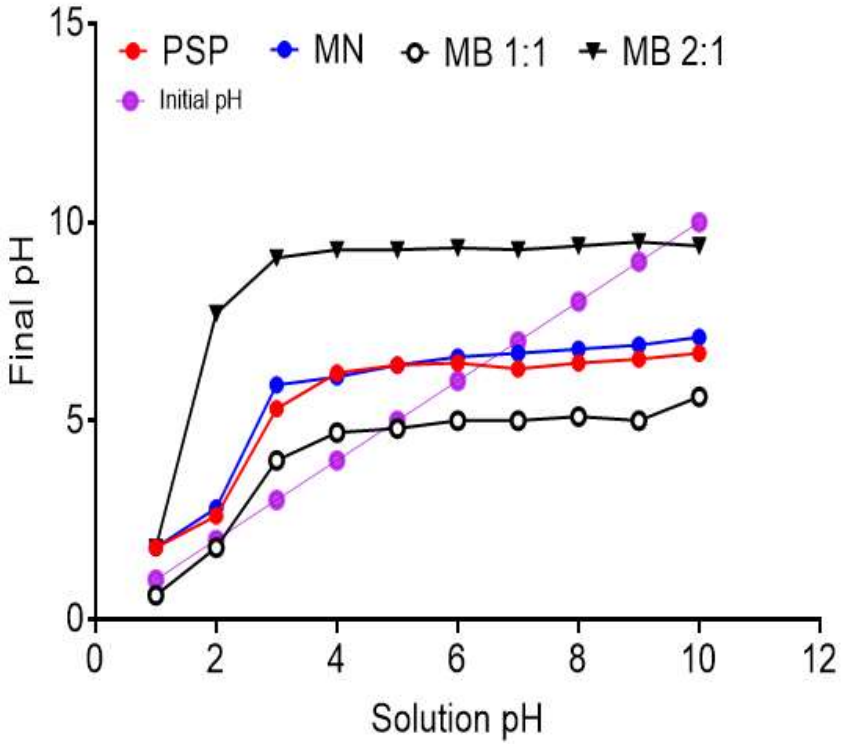

Figure 8: Determination of point zero charge of the samples

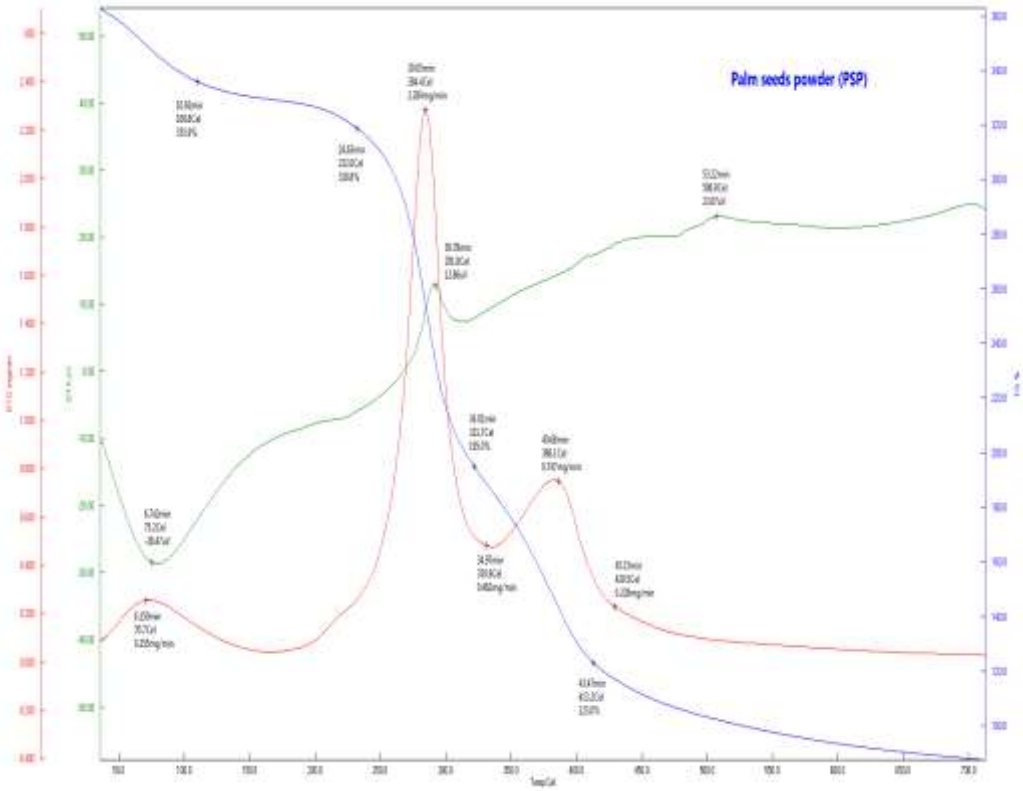

Figure 9: TG curves of PSP from 50 to 800 ^{o}C

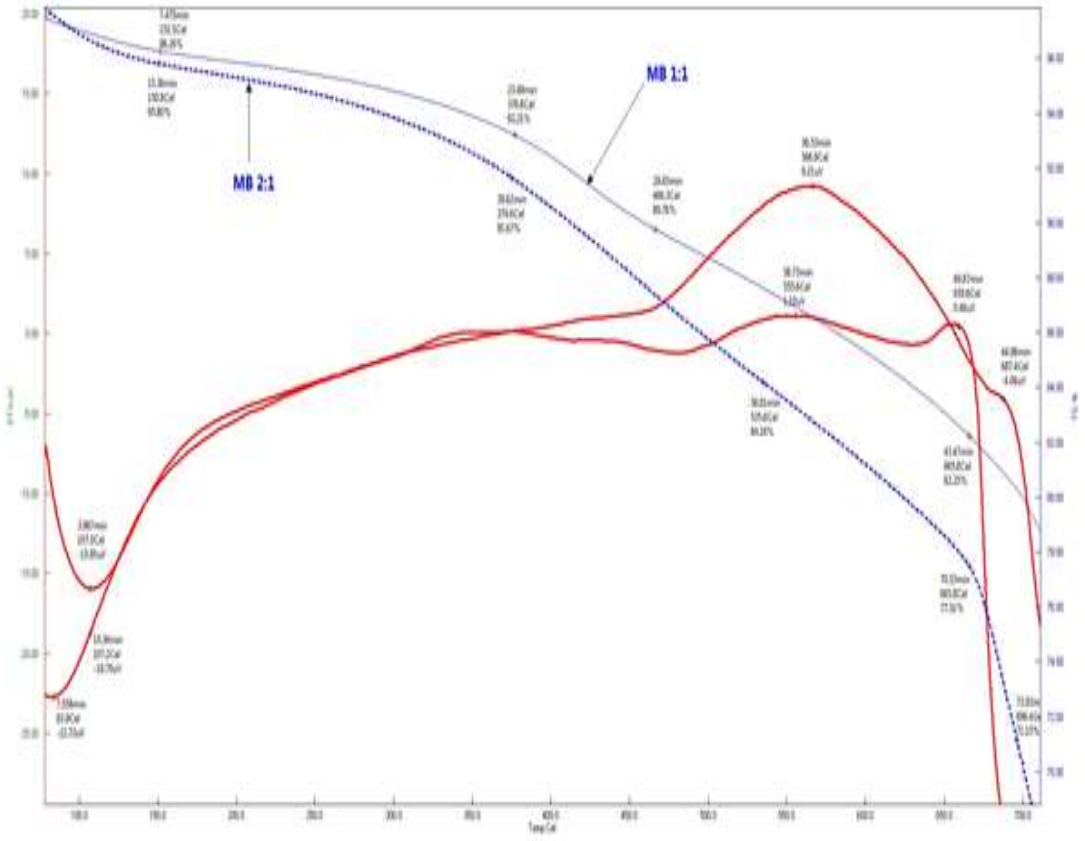

Figure 10: TGA of MB 1:1 and MB 2:1

The thermal decomposition of the samples is shown in Fig. 9. For PSP material, the TGA curve descends from 50 ^{o}C until it becomes horizontal around 500 ^{o}C, and approximately 69% weight loss was recorded during the thermal process. The TGA–DTA traces indicate three major domains having a rapid water loss between 50 ^{o}C to 100 ^{o}C which is about 25.5% of initial PSP weight. The second weight loss from 250 ^{o}C to 350 ^{o}C (34.2%) is ascribed to the decomposition of chemically bound groups. The third step occurred from 350 ^{o}C to 500 ^{o}C (9.3%) is related to degradation of carbon moiety in the PSP material. The DTG curve shows two small broad peaks and a sharp peak in the range of temperature about 70–400 $^{\circ}$C which indicate endothermic process (Ding et al., 2016).

On the other hand, TGA curves of both MB mass ratios 1:1 and 2:1 samples gave the same decomposition trend at the beginning of the thermal process (Fig.10). The TGA of the MB shows four weight loss stages during the thermal process. The first degradation stage observed around 50 to 100 ^{o}C is related to moisture loss. The weight loss determined in this step is 3.74% and 4.2% for MB 1:1 and MB 2:1, respectively. It is evidently clear that biochars are mechanically stronger and stable compared with palm seeds powder material. Meanwhile, MB 1:1 shows more thermal stability in comparison to MB 2:1. For this reason, all adsorption experiments were performed with MB 1:1.

4.2 Evaluation of adsorbents capacity

Various adsorbents ratios were prepared and their uptake capacities were evaluated using 100 mg/L of initial concentration and 0.5g of adsorbent. As observed, MB 2:1 exhibited highest removal efficiency (Fig.11) as compared with MB 1:1 and MB 1:2. Despite the MB 2:1 adsorptive potential, its magnetic recoverability and thermal stability is lower in comparison to MB 1:1. Hence, MB 1:1 was used for all the experimental studies.

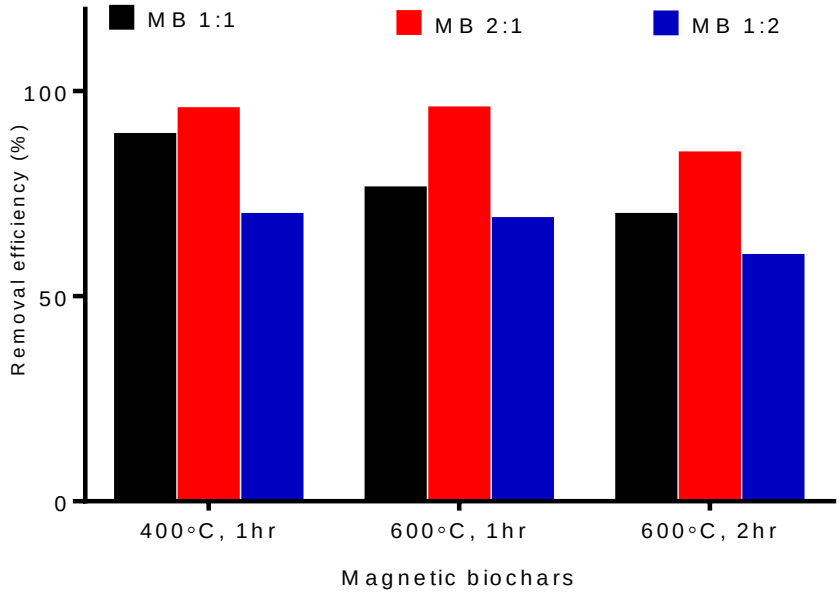

Figure 11: Evaluation of adsorbents uptake capacity

4.3 Impact of operation parameters on nickel removal

4.3.1 Effect of solution pH

The influence of the solution pH on the uptake of nickel from aqueous solution was investigated. The maximum nickel uptake occurred at pH 3 (12 mg/g), that is about 93% of Ni^{2+} was removed at the acidic domain by the magnetic biochar. As observed, pH 4.0 to 6.0 has less effect on nickel uptake (Fig.12), while beyond pH 7 a further decrease was observed which could be attributed to the formation of hydroxides by the nickel (Oladipo and Gazi, 2015). As reported by Lam et al., (2016) the predominant nickel species beyond pH 8 is $Ni(OH)_2$. Hence, the formation of aqueous nickel hydroxide probably limits the uptake of nickel by MB beyond pH 7.

The observed trend of the pH followed the concept of pH_{pzc}. Thus, the removal efficiency observed between pH 3 and 7 is explained based on the surface chemistry of the MB. As earlier stated, the pH_{pzc} of MB is determined as 2 and 5, hence, the surface of the MB becomes negative when the solution pH is higher than the pH_{pzc}.

During this stage, the positively charged nickel ions become electrically attracted to the MB surface (Kooh et al., 2016).

The final solution pH was also determined as shown in the Fig.12. Beyond pH 5, the final pH was observed to be lower than the initial pH. This observation may be attributed to the release of protons (H^+) into the solution as the nickel ions are being exchanged on the surface of the magnetic adsorbent. Thus, we concluded that ion-exchange might also play a role in the nickel removal process by MB. The Similar observation had been reported by (Kannan and Thambidurai, 2008).

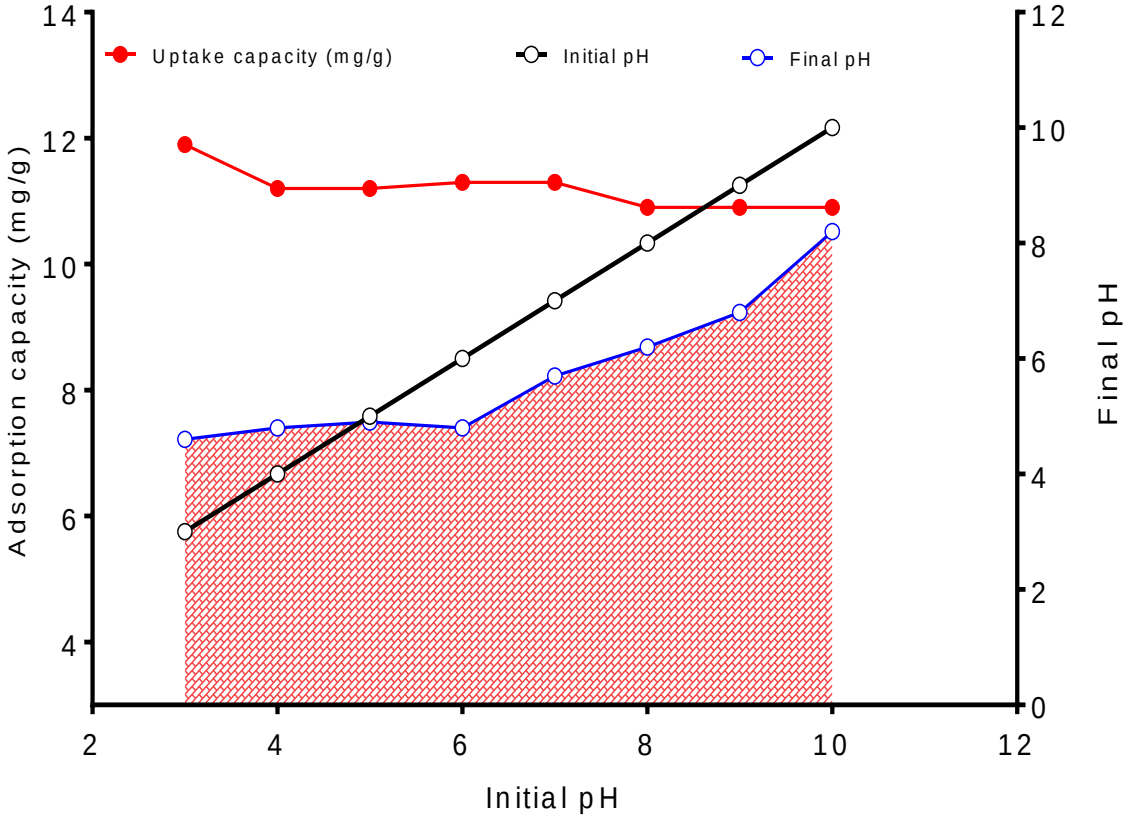

Figure 12: Effect of solution pH on Nickel removal by MB

4.3.2 Effect of temperature and initial concentration of nickel

The influence of initial Ni^{2+} ion concentration is shown in Fig. 13. This figure reveals that the quantity of nickel ions adsorbed increases rapidly with increases in the initial concentration from 1 mg/L, and then gradually decreases until equilibrium is attained at concentration 100mg/L. No significant removal percentage was recorded beyond 100 mg/L. In lower concentration; the ratios of active surface sites to the total ions in the solution is high; hence, all ions may interact with the active functional groups on the surface of the adsorbent and be removed from the solution. However, at higher concentration, the numbers of metal ions are relatively higher than binding sites. Thus, a lower adsorption capacity is observed (Ghasemi et al. 2014; Matouq et al. 2015).

Besides, the effect of temperature on nickel removal was investigated at different temperature (25 ^{o}C–80 ^{o}C). Increased nickel uptake was noticed with increases in solution temperature. This could be as a result of increased diffusion of nickel molecule into the internal pores of the adsorbent, leading to increased uptake of the metal ions (Sheshdeh et al. 2015; Matouq et al., 2014). At 25 ^{o}C the amount of nickel adsorbed was 15 mg/g, and with increases in temperature (65 ^{o}C), the uptake reached 27 per unit mass of MB. It is important to stress that, a slight increase in nickel uptake was observed as the temperature increased to 80 ^{o}C.

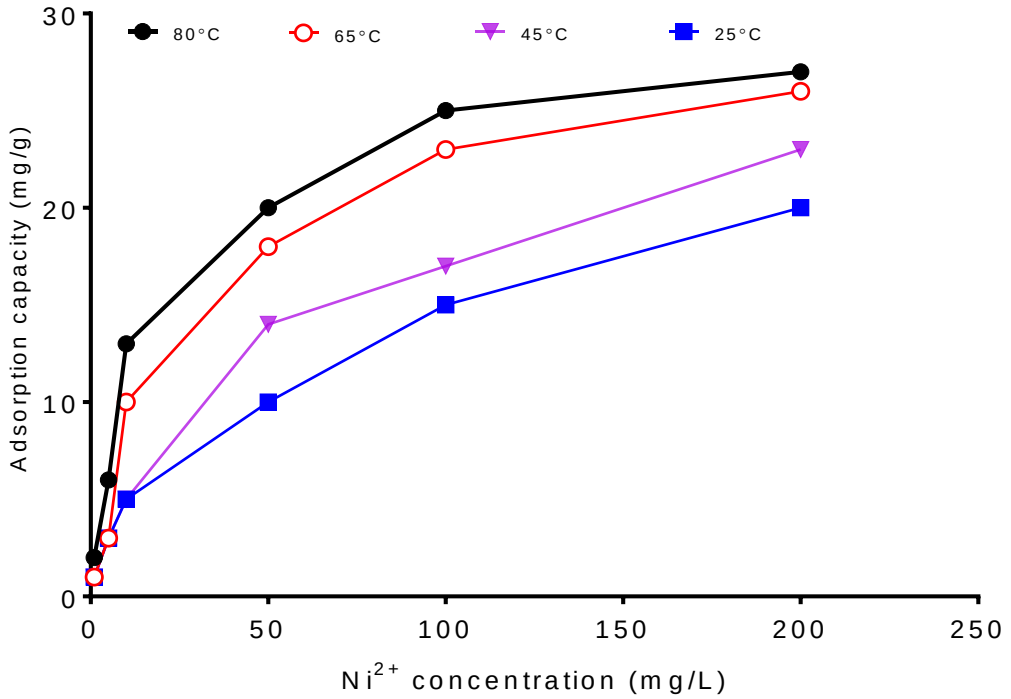

Figure 13: Effect of temperature and initial concentration of Nickel removal by MB

4.3.3 Effect of contact time

The rate of Ni^{2+} ions removal by the magnetic biochar was investigated. Fig.14 illustrates the impact of contact time in the adsorption capacity of nickel from aqueous solution using MB. At the constant concentration, the amount of adsorbed nickel ions was fast initially and increased gradually until equilibrium attained at 100min and 28mg/g uptake recorded. Beyond 100 min, no significant uptake was observed. The rapid adsorption rate at the beginning of the adsorption process can be ascribed to the presence of vacant sites. As the time proceeds, the adsorbed of Ni^{2+} ions will block the exterior surface of the adsorbent; this might limit the rate of adsorption (Lam et al., 2016).

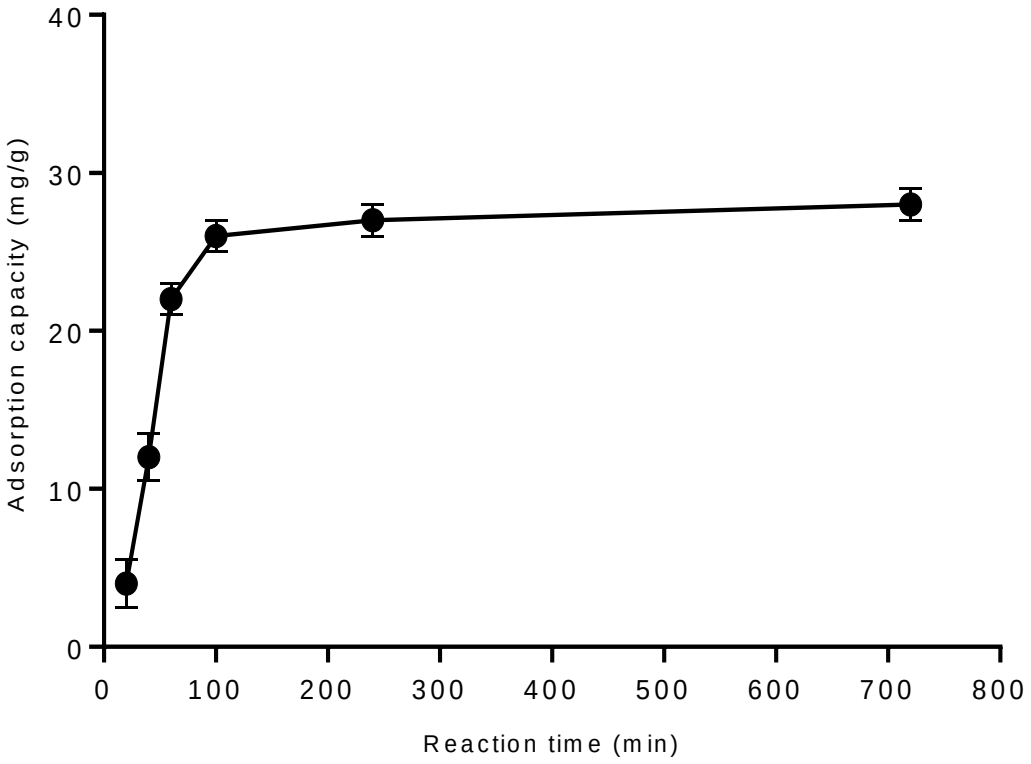

Figure 14: Effect of contact time on Nickel removal by MB

4.3.4 Effect of adsorbent dose

As shown in Fig. 15, the adsorption capacity for Ni^{2+} ions decreased from 29 to 5 per unit mass of adsorbent, as the MB dose increases from 0.25g to 1.0 g. This reduction could be as a result of adsorbent agglomeration and possible competition between adsorbed and incoming metal ions. Contrarily, the percentage of nickel removed increased from 24% to 65% as the amount of adsorbent increased from 0.25 to 1.0g. This can be attributed to increasing surface area and rapid migration of adsorbate molecules from the aqueous media to the available sorption-active sites (Lam. 2016, Oladipo and Gazi. 2015).

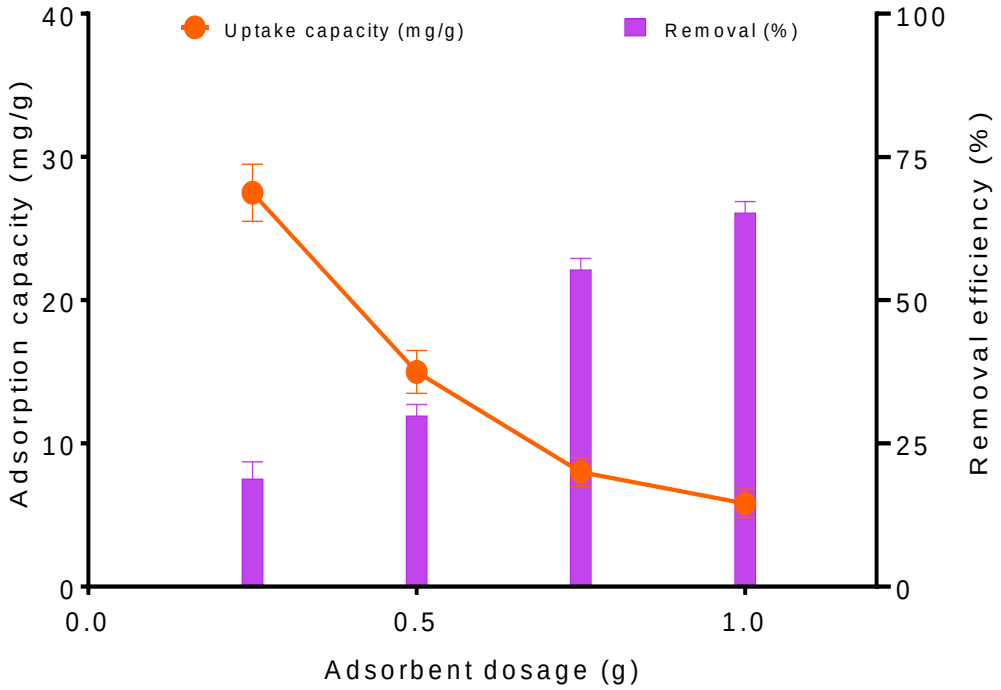

Figure 15: Effect of adsorbent dosage of Nickel removal by MB

4.3.5 Effect of competing ions

The MB adsorption efficiency was checked in the presence of competing ions as real wastewaters usually contain various co-existing pollutants. As observed, the uptake of nickel ions by MB decreased with increasing concentration of coexisting ions (copper, manganese, and Rhodamine B dye). As shown in Fig.16, in the absence of the multi-pollutant the removal efficiency of nickel was high (>91%). On the other hand, in the presence of 0.5mg/L of copper and manganese, the percentage of nickel removed decreased sharply from the 91% to 45% and 55% respectively. Interestingly, only 16% reduction was observed in the presence of 0.5mg/L Rhodamine B (Rb). A decreasing trend was recorded as the concentration of the co-pollutants increased. This could be ascribed to competition for sorption sites by Ni^{2+} ions and the positively charged co-existing species (Kooh et al., 2016).

The Rb has less effect on the MB uptake capacity and could due to the large molecular weight of Rb (442.6 g/mol) as compared to that of nickel (58.7 g/mol). Thus, when both adsorbates were present in the solution, the higher mobility of nickel may have outweighed the heavy Rb, resulting in less inhibitive interaction and higher diffusivity of Ni^{2+} (Oladipo and Gazi. 2016).

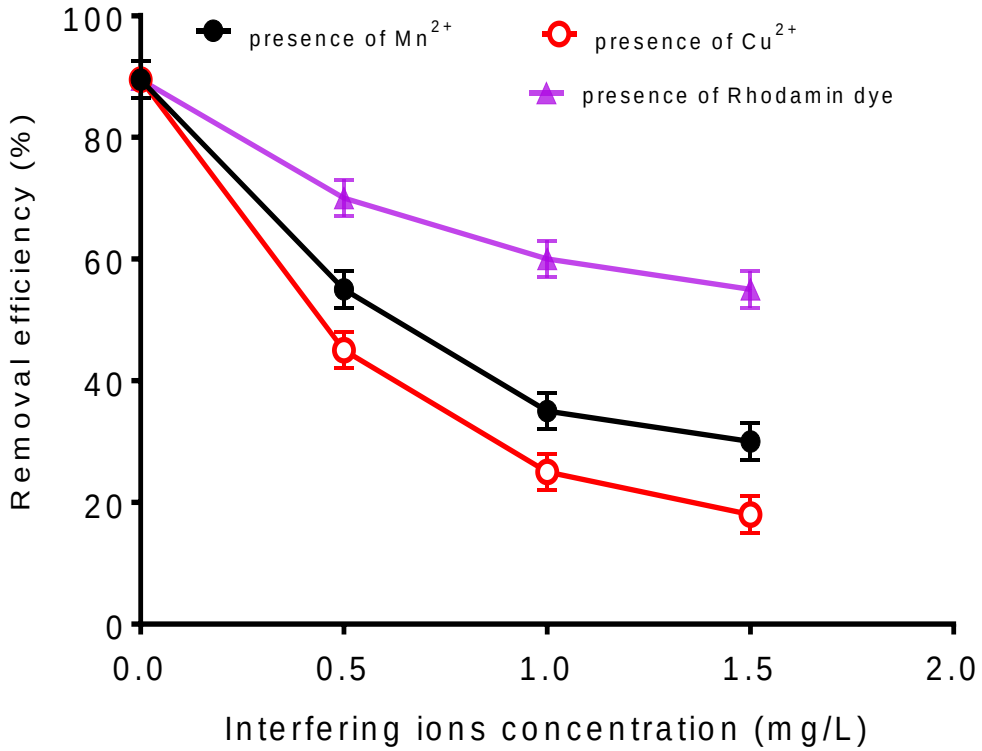

Figure 16: Effect of competing ions on the removal of Ni^{2+} ions by MB

4.3.6 Effect of salinity

The effect of ionic strength on the Ni^{2+} adsorption process was investigated. Fig.17 shows the influence of sodium chloride concentration on the removal efficiencies of nickel. In the absence of salt, the Ni^{2+} ion removal efficiency reached 90%. However, when 0.5g/L of NaCl was introduced into the medium, the removal efficiency decreased rapidly to 70% which is about 20% reduction in capacity. It is observed

that when the concentration of NaCl increased to1.0 g/L, only a slight decline of 10% was observed. The removal efficiency remained stable even when the sodium chloride concentration was increased from 1.0 to 2.0g/L. The reduction of nickel uptake with increasing ionic strength of the medium could be as a result of suppressive influences on electrostatic interaction between Ni^{2+} and Na^{+} (Hu et al., 2013: Kooh et al., 2016). The accumulations of Na^{+} on the external surface of MB resulted to high amount of net positive charge. Subsequently, repulsion between the Ni^{2+} and adhered Na^{+} occurred, hence lowering the uptake capacity of MB. Similar trends have been reported (Oladipo et al., 2014; Oladipo and Gazi, 2015; Villaescusa et al., 2000).

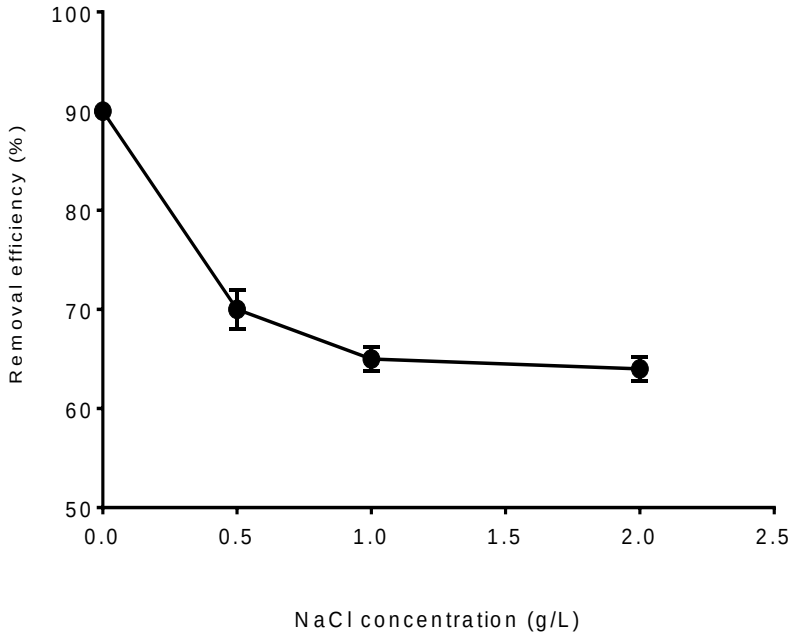

Figure 17: Effect of NaCl on Nickel removal by MB

4.4 Isotherms adsorption studies

Isotherm offers insights into the interactive relationship between the adsorbate and the adsorbent. Five models were utilized to explain the sorption behavior of the MB

at different reaction temperature as depicted in Table 4. The isotherm parameters were obtained from the plot of the amount of nickel adsorbed at equilibrium (q_e) versus the equilibrium concentration of the metal ions (C_e) as shown in Fig. 18a–d.

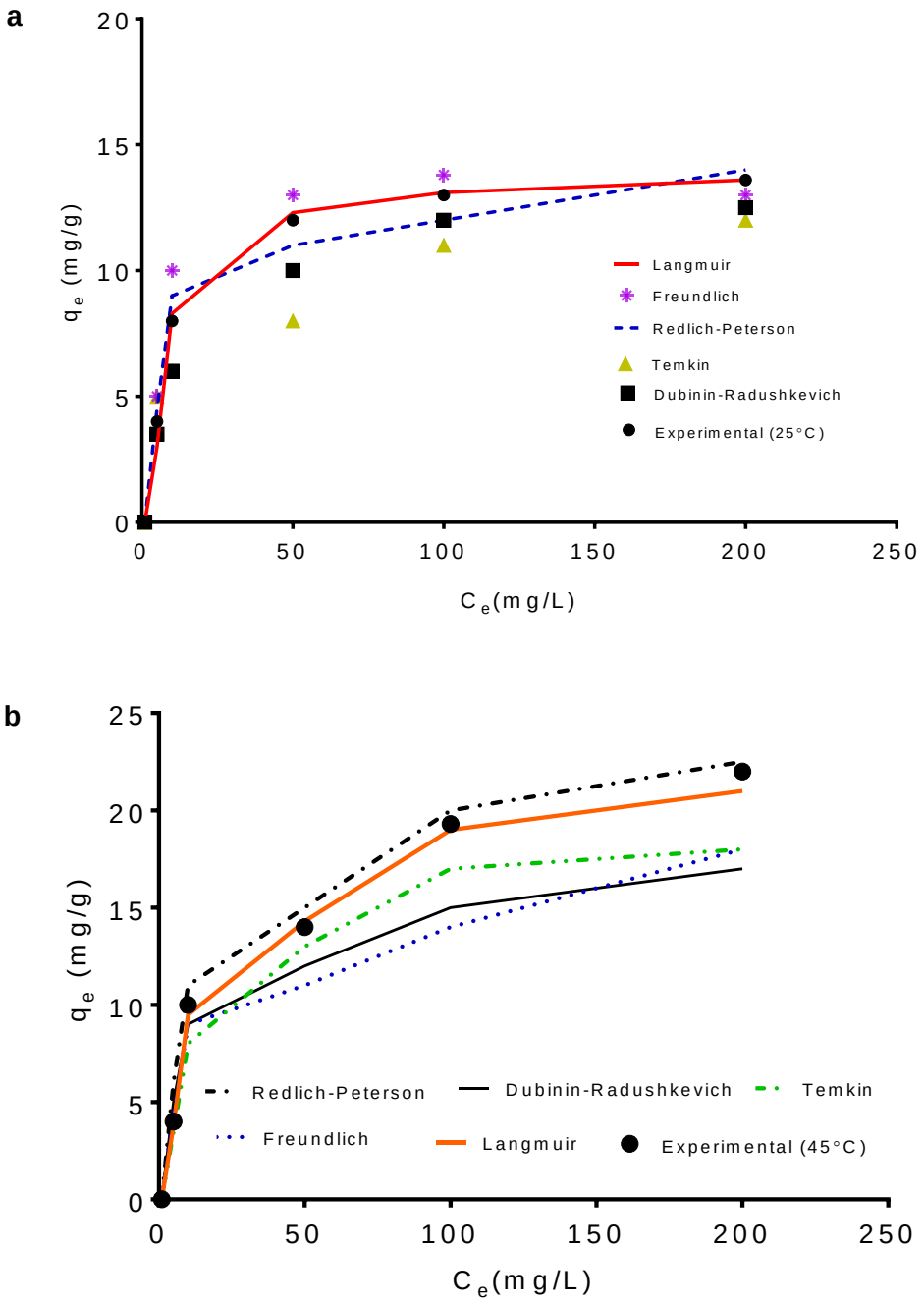

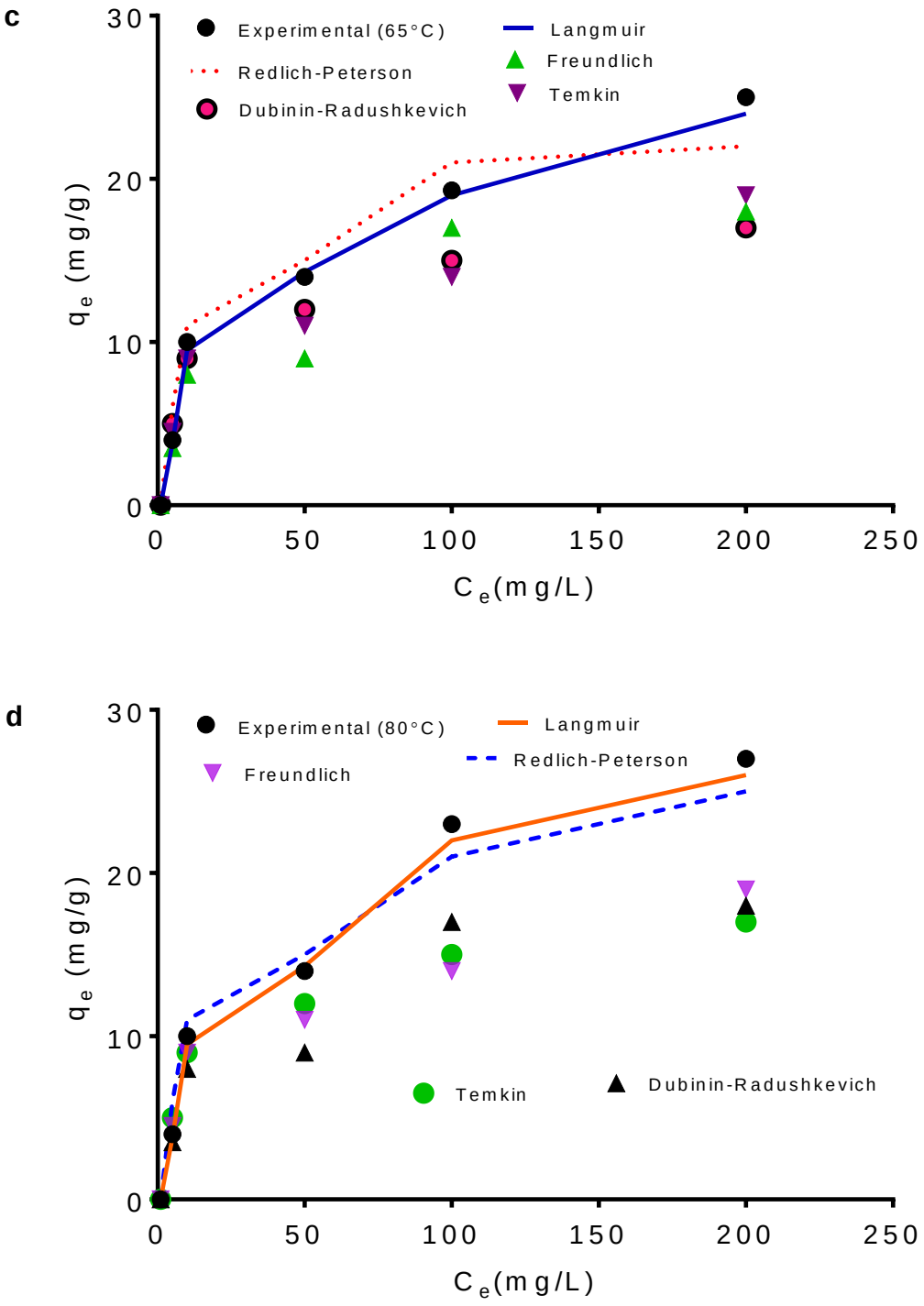

Figure 18 a–d: Adsorption isotherms of Ni^{2+} ions onto MB at various temperatures

As tabulated, the uptake capacity for Ni^{2+} ions increased from 17.4 to 27.8 mg/g with increasing temperature from 25˚C to 80˚C. Increases in temperature enhanced the surface activity and pores of the adsorbents with subsequent increases in the adsorbate kinetic energy, thereby resulting in higher removal efficiency.

Table 4: Isotherm parameters for nickel adsorption at different temperature

Model	**Parameter**	**Temperature (^{o}C)**			
		25	**45**	**65**	**80**
Langmuir	q_m (mg/g)	17.4	22.8	26.1	27.8
	K_L (L/mg)	0.072	0.126	0.156	0.144
	R_L	0.0649	0.0381	0.0311	0.0336
	χ^2	0.0133	0.0551	0.0455	0.0252
	R^2	0.997	0.999	0.999	0.998
	SAE	8.5	9.4	7.9	6.9
Freundlich	K_F (mg/g(L/mg)$^{1/n}$)	2.59	2.13	1.95	1.78
	n	2.78	2.45	2.23	1.99
	χ^2	0.783	0.652	0.741	0.698
	R^2	0.955	0.919	0.929	0.972
	SAE	10.1	11.3	9.9	10.4
Temkin	A	2.38	1.87	1.03	0.932
	b	19.8	20.3	21.6	21.4
	χ^2	0.0839	0.0934	0.0609	0.0952

	R^2	0.993	0.981	0.989	0.982
	SAE	10.9	11.8	9.3	13.8
D–R	q_m (mg/g)	16.3	19.7	22.6	23.3
	E (kJ/mol)	6.89	9.45	7.89	11.99
	K_{DR} (mol^2/kJ^2)	6.91	10.5	13.9	22.6
	χ^2	0.0733	0.0799	0.0609	0.0652
	R^2	0.963	0.941	0.989	0.992
	SAE	12.9	10.9	8.9	11.8
R–P	g	4.92	5.63	6.45	4.98
	a_R	0.0344	0.120	0.0931	0.119
	β	0.995	0.986	0.899	0.909
	χ^2	0.0937	0.0995	0.0809	0.0952
	R^2	0.993	0.999	0.992	0.997
	SAE	6.8	5.9	8.9	9.2

The trend indicates that the adsorption is an endothermic process (Sheshdeh et al., 2014). The degree of fittings of the isotherms was assessed using correlation coefficient (R^2), the sum of average errors (SAE) and Chi-square (χ^2). A higher value of R^2 near unity, lower values of SAE and χ^2 indicate adequate representation of experimental data by the isotherms. The *n* values of the Freundlich isotherm at different temperature are greater than unity which indicated that the adsorption is favorable. The adsorption of Ni^{2+} ions by MB followed the Langmuir model, since the model exhibited the highest R^2 value and the lowest SAE value.

In addition, the R_L value of the Langmuir model falls between 0 and 1 which indicates favorable adsorption. The mean free energy of adsorption process obtained from the D-R isotherm model the range between 8 to 16 kJ/mol. Therefore, we concluded that the uptake of Ni^{2+} ions by MB is probably via chemical or ion exchange process. Similar reports have been given by (Matouq et al. 2015, Sheshdeh et al. 2014). The maximum amount of Ni^{2+} adsorbed in this research is compared with reported uptake under various operating conditions (Table 5).

Table 5: Maximum adsorption capacity of various adsorbents for Ni^{2+}

Adsorbents	**pH**	**C_o (mg/L)**	**q_m (mg/g)**	**Reference**
NaOH-Mangifera	6.0	800.0	131.5	Nadeem et al., 2014
n-HApAg	7.0	200.0	360.2	Oladipo and Gazi, 2015
AB	7.0	100.0	199.5	Oladipo and Gazi, 2014
AC	6.0	100.0	8.641	Sun et al., 2014
Chitosan CS-MA	5	10	0.87	Heidari et al., 2013
Chitosan	5	500	120.5	Srinivasa et al., 2009
RM	7.5-7.9	250	10.95	Lopez et al., 1998
MB	3.0	100	27.8	**This study**
Chitosan/magnetic composite beads	6	70	52.55	Tran et al., 2010
Granular biomass	5	35.5	26.0	Hawari and Mulligan, 2006

4.5 Kinetic studies

The performance rate of the adsorbent was investigated using earlier mentioned kinetic models according to Eqs. 1–4 respectively (Laus et al., 2010). The amount of Ni^{2+} adsorbed (q_e) onto MB at time t, and the rate constant (k) were calculated, and

the other related parameters are listed in Table 6. From the table, it is clear that the PSO has the highest correlation coefficient values (R^2) (0.996–1.000) and the smallest values of the error functions (3.81–6.98) as compared with other models. Additionally, the $q_{e,cal}$ value is close to $q_{e,exp}$ value; 2.2 and 2.4mg/g, respectively. This confirms that the uptake of Ni^{2+} ions onto MB follows PSO model in all cases, confirming the sorption process is chemically controlled with possible sharing or exchange of ions between Ni^{2+} and MB (Laus et al., 2010).

It is observed that the results obtained from the kinetic studies agree with those of isotherm and similar observations have been recorded for nickel removal using Mangifera indica waste biomass and alginate-based composite (Oladipo and Gazi, 2015; Nadeem et al., 2014). Three possible mechanisms occur during an adsorption process. However, the PFO and PSO cannot explain the diffusion mechanism of adsorbate into the internal pores of the adsorbent. Hence, the experimental data were further analyzed using the intra-particle diffusion model.

Table 6: Kinetic parameters for nickel adsorption using MB

		Initial concentration (mg/L)			
Model	**Parameter**	**5**	**10**	**50**	**100**
Pseudo-first-order	$q_{e,exp}$ (mg/g)	2.4	8.8	16.1	24.8
	$q_{e,cal}$ (mg/g)	4.9	5.3	22.1	20.9
	k_1 (1/min)	0.0149	0.0205	0.0366	0.0132
	χ^2	0.0833	0.0951	0.0755	0.0992
	R^2	0.983	0.967	0.955	0.912
	SAE	10.5	12.4	9.91	10.9
Pseudo-second-order	$q_{e,exp}$ (mg/g)	2.4	8.8	16.1	24.8
	$q_{e,cal}$ (mg/g)	2.2	6.3	17.9	22.9
	k_2 (1/min)	0.542	0.481	0.311	0.206
	χ^2	0.0103	0.0251	0.0155	0.0452
	R^2	0.999	1.000	0.999	0.996
	SAE	3.81	4.98	5.89	6.98
Elovich	β (g/mg)	1.88	1.37	1.09	0.911
	α (mg/g min)	15.8	23.8	33.6	29.4
	χ^2	0.0839	0.0934	0.0609	0.0952
	R^2	0.994	0.993	0.987	0.999
	SAE	3.93	7.82	3.32	4.89
Intraparticle diffusion					
First region	C_a	9.89	11.4	17.9	21.9
	k_a (mg/g $min^{1/2}$)	2.98	3.12	4.90	5.61
	χ^2	0.0433	0.0391	0.0488	0.0592
	R^2	0.999	1.000	0.997	0.934
	SAE	14.9	16.9	18.9	11.9
Second region	C_b	24.9	35.63	66.45	74.98
	k_b (mg/g $min^{1/2}$)	0.036	0.134	0.0142	1.19
	χ^2	0.0137	0.0211	0.0312	0.0252
	R^2	1.000	0.948	0.891	0.999
	SAE	16.8	14.9	12.9	15.5

The adsorption rate was plotted against the reaction time to obtain the parameters of PSO, PFO and Elovich models as shown in Fig. 19. The intra-particle diffusion will be the rate controlling step, if the plot of q_t against $t^{1/2}$ gives a linear plot that passes through the origin (Weber and Morris 1963). However, when the straight line does

not pass through the origin, indicates the adsorption rate is possibly controlled by other mechanisms. According to Fig. 20, intra-particle model was not the only rate–limiting mechanism (Erol and Ozdemir., 2016).

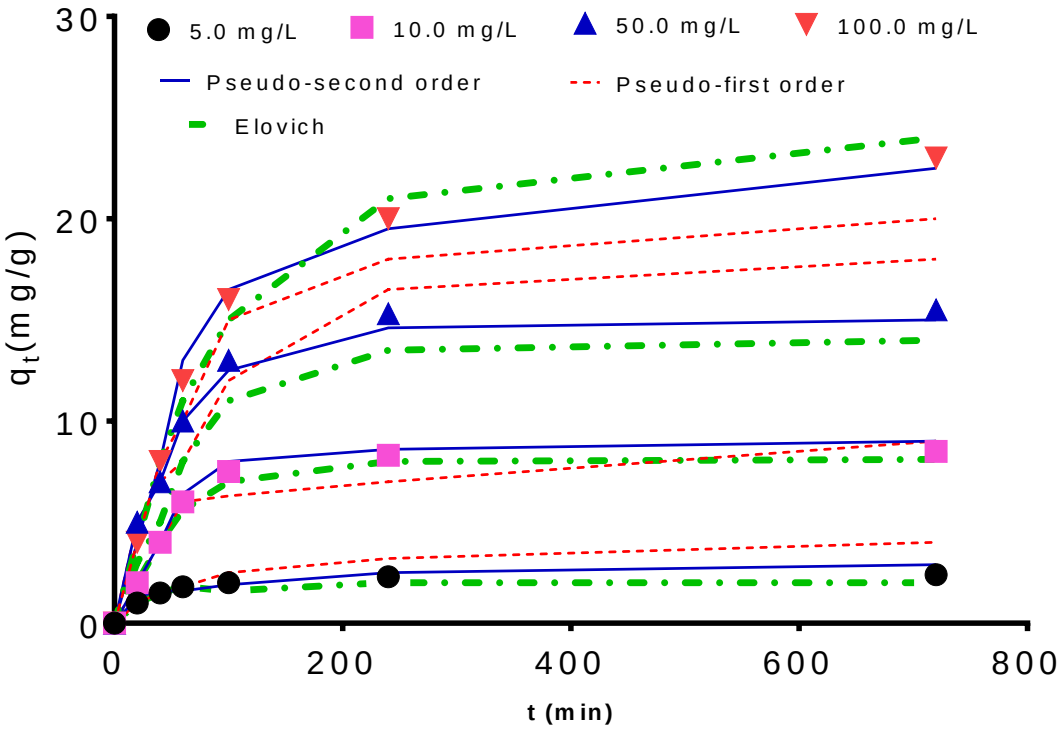

Figure 19: Comparison of kinetic models at different initial nickel concentrations

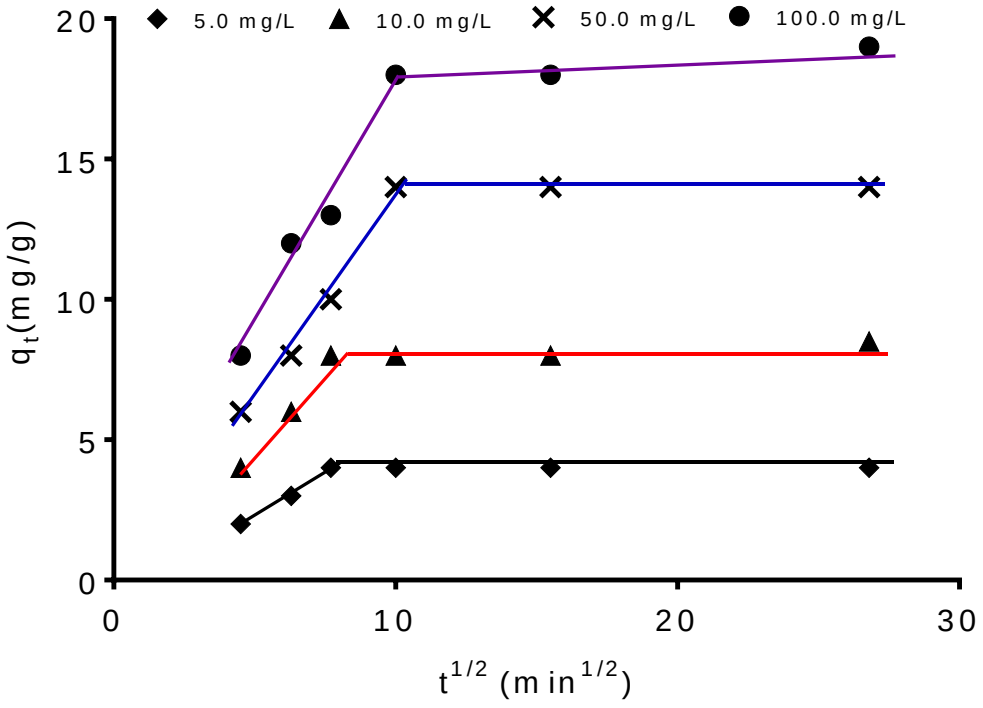

Figure 20: Intra-particle plot of nickel removal by M

4.6 Sorption thermodynamic

The thermodynamic parameters such as the Gibbs free energy change (ΔG), enthalpy change (ΔH), and entropy change (ΔS) were obtained at different temperatures (25, 45, 65, and 80˚C) and initial concentrations (5-100 mg/L) using Van't Hoff equations to find these variables:

$$\Delta G = -RT \ln k \quad (12)$$

$$\Delta G = \Delta H - T\Delta S \quad (13)$$

$$k = \frac{C_s}{C_e} \quad (14)$$

Where, k is the distribution coefficient, Cs (mg/L) is quantity of the (Ni^{2+}) adsorbed, the gas constant is R (J/mol k), T is the absolute temperature (k).

As illustrated in Table 7, ΔH and ΔS values are positive and ΔG values are negative. The negative ΔG indicates spontaneous interaction between the Ni^{2+} and the MB. The positive values of ΔH and ΔS indicate endothermic adsorption process between Ni^{2+} and MB, and a decrease in randomness at the adsorbent interface during the adsorption process, respectively (Kooh et al., 2016). Also, a decreasing trend is observed in the ΔG with rises in temperature, indicating favorable adsorption at higher temperature. This observation is in line with Langmuir model tabulated (Table 4).

Table 7: Thermodynamic parameters for the Nickel adsorption using MB

Parameter			ΔG (kJ/mol)			
C_o(mg/L)	ΔH (kJ/mol)	ΔS (kJ/mol K)	25°C	45°C	65°C	80°C
5	2.65	0.0861	-23.1	-24.7	-26.5	-27.7
10	2.35	0.0832	-22.4	-24.1	-25.8	-27.1
50	2.11	0.0789	-21.4	-22.9	-24.6	-25.7
100	1.98	0.0678	-18.2	-19.6	-20.9	-21.9

4.7 Regeneration and reuse

To examine the stability and reusability potential of the MB for economical purposes regeneration studies were performed. 0.5g of Ni^{2+} loaded-MB was placed into 20mL of different desorption reagents (0.1M HCl, 0.1M H_2SO_4, 0.1M NaOH, and H_2O) and mechanically agitated for 2h. A consecutive desorption–adsorption runs were performed for each elution agent. The desorption capacity was defined as the ratio of the mass of Ni^{2+} regenerated to the mass of the metal adsorbed (Oladipo and Gazi. 2015).

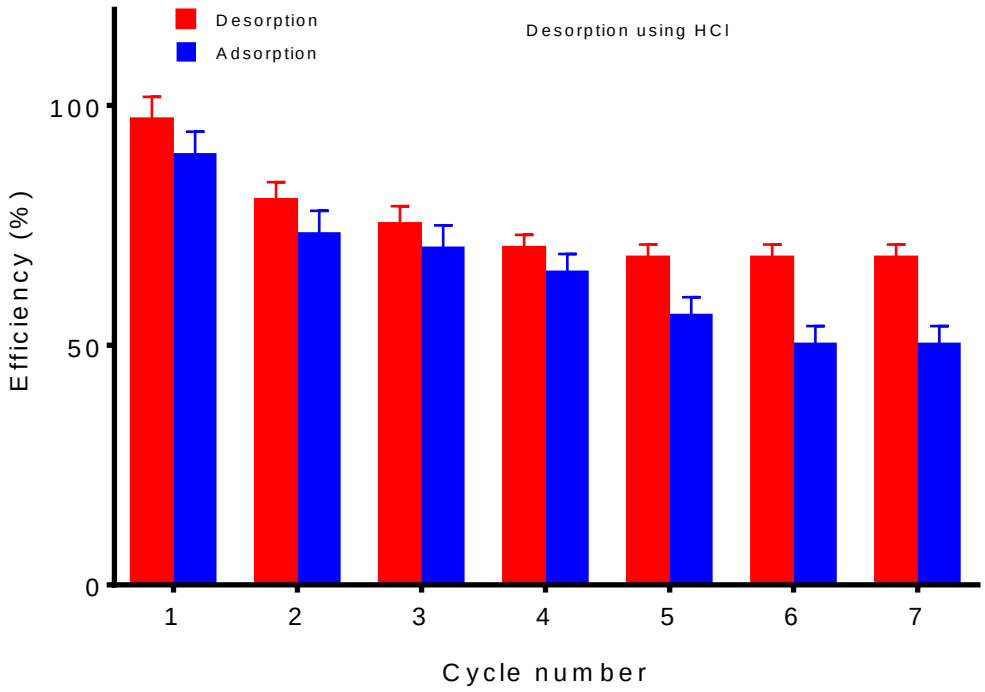

Figure 21: Adsorption-desorption using HCl reagent.

From the figures 21–24, it was found that HCl shows the highest regeneration efficiency (97%) as compared with the other reagents which performed moderately (about 77%) for H_2SO_4 and H_2O. The NaOH exhibited very low desorption capacity (45%). The maximum Ni^{2+} regeneration was observed in the acidic medium (HCl), ascribed to increases in the number of protons in the medium, and subsequent competition between H^+ and adsorbed Ni^{2+} ions on the same active sorption sites. However, some adsorbed Ni^{2+} ion are strongly bound to MB leading to a decrease in the desorption capacity. In the basic medium (NaOH), the minimum desorption percentages observed could be attributed to the large size of Ni^{2+} ions compared to Na^{2+} ions. Hence, it is difficult to Na^{2+} ions to replace Ni^{2+} ions on the active sorption sites on MB.

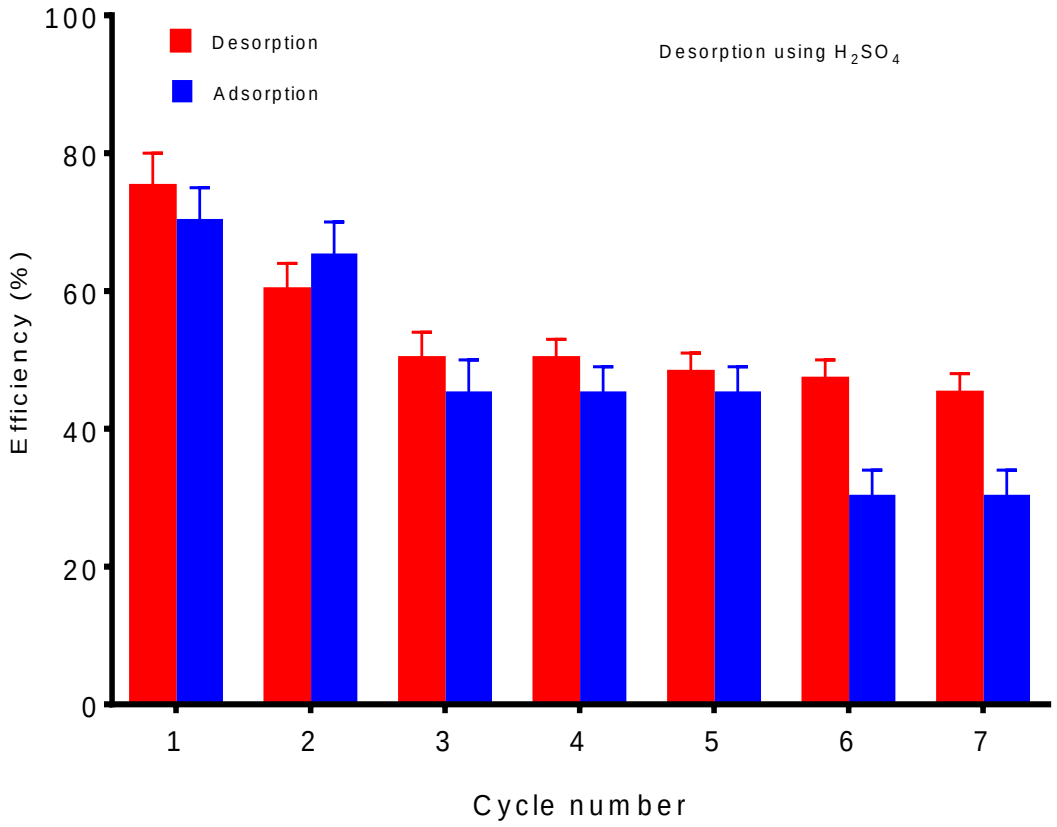

Figure 22: Adsorption-desorption using H_2SO_4 reagent

Also, presence of NaOH will increase the pH of the system, and then increase the negativity of the adsorbent surface. Hence, electrostatic attraction of negatively charged MB and positively charge Ni^{2+} ions decreases the desorption process. After the seven cycles, the uptake capacity of MB decreased from 90% to 55%, where recovery of Ni^{2+} in 0.1 $molL^{-1}$ HCl decreased from 96% in the first cycle to 65% in the fourth cycle, and the desorption remains constant from this cycle to the last one. However, the adsorption capacity decreases further even after the fourth cycle. According to those results, it can be concluded that MB is a good adsorbent and can be used and reused successfully for more than seven cycles (Lam et al., 2016).

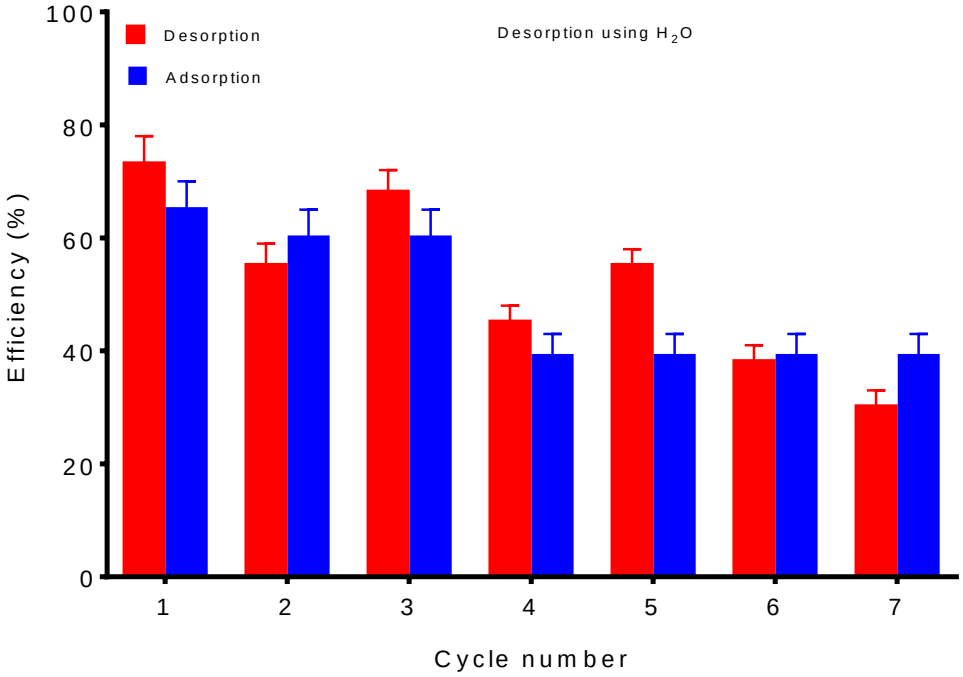

Figure 23: Adsorption-desorption using H_2O reagent

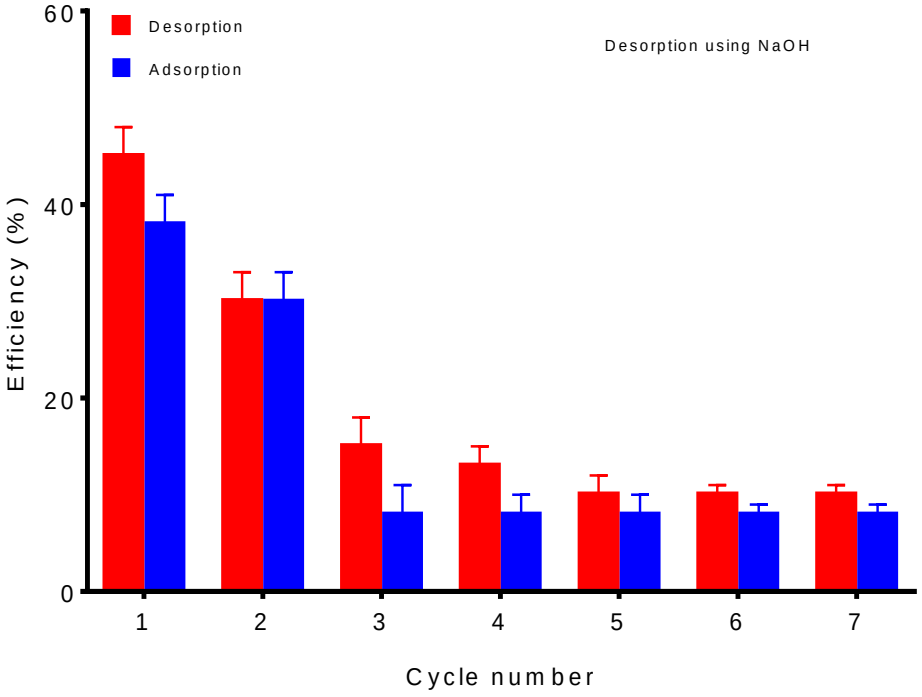

Figure 24: adsorption-desorption using NaOH reagent

Chapter 5

CONCLUSION

In this research, the performance of magnetic biochar prepared from palm seeds has been investigated for nickel removal from the aqueous medium. Physiochemical characterization of the adsorbent was performed. The analysis of all experimental results reveals the following:

- The removal efficiency of MB was influenced by various parameters (pH solution, contact time, adsorbent dosage, and temperature.
- Maximum uptake occurred at pH 3.
- The removal efficiency increased steadily with increases in temperature which indicates an endothermic sorption process.
- Langmuir model evidently described the sorption behavior of MB and Ni^{2+} with high correlation coefficient R^2 (0.997–0.999) and very low error values, χ^2 (0.0133–0.0551).
- The adsorption rate is either chemically controlled or ion exchange and intra-particle diffusion played a role in the process.
- Thermodynamic results showed that the adsorption process is spontaneous and endothermic in nature.
- The MB can withstand successive use and reuse without considerable loss of stability or activity.

REFERENCES

Asati, A., Pichhode, M., & Nikhil, K. (2016). Effect of heavy metals on plants: An Overview. *International Journal of Application or Innovation in Engineering & Management (IJAIEM). 2319-4847.*

Bailey, S., Olin, T., Bricka, R., & Adrian, D. (1999). A review of potentially low cost Sorbents for heavy metals. *Wat. Res., 33(11), 2469-2479.*

Barakat, M.A. (2010). New trends in removing heavy metals from industrial wastewater. *Arabian Journal of Chemistry, (4), 361-377.*

Barton, J., Garcia, M., B., G., Santos, D., H., Fanjul-Bolado, P., Ribotti, A., McCaul, M., Diamond, D., & Magni, P. (2016). Screen- printed electrodes for environmental monitoring of heavy metal ions: a review. *Microchim Acta, (183), 503-517.*

Cempel, M., Nikel, G. (2006). Nickel: A review of its sources and environmental toxicology. *Polish J. of Environ. Stud, (15), 375-382.*

Chen, X., Chen, G., Chen, L., Chen, Y., Lehmann, J., McBride, M., B., & Hay, A., G. (2011). Adsorption of copper and zinc by biochars produced from pyrolysis of hardwood and corn straw in aqueous solution. *Bioresource Technology, (102), 8877-8884.*

Ding, Z., Hu, X., Wan, Y., Wang, S., & Gao, B. (2016). Removal of lead, copper,

cadmium, zinc, and nickel from aqueous solutions by alkali-modified biochar: Batch and column tests. *Journal of Industrial and Engineering Chemistry, (33), 239-245*.

Duda-Chodak, A., & Blaszczyk, U. (2008). The impact of nickel on human health. *J. Elementol,13(4),685-696.*

El-Sadaawy, M., & Abdelwahab, O. (2014). Adsorptive removal of nickel from aqueous solution by activated carbons from doum seed (Hyphaenethebacia) coat. *Alexandria Engineering Journal, (53), 399-408.*

Erol, S., & Ozdemir, M. (2014). Removal of nickel from aqueous solution using magnetic tailing. *Desalination and Water Treatment, (57:13), 5810-5820.*

Ghasemi, M., Ghasemi, N., & Azimi-Amin, J. (2014). Adsorbent ability of treated peganum harmala-L seeds for the removal of Ni (II) from aqueous solutions: Kinetics, Equilibrium and Thermodynamic studies. *Indian Journal of Materials Science, 459-674.*

Gupta, V., K., Mittal, A., & Gajbe, V. (2005). Adsorption and desorption studies of a water soluble dye, Quinoline Yellow, using waste materials. *Journal of Colloid and Interface science, (284), 89-98.*

Hawari, A. H., & Mulligan, C. N. (2006). Biosorption of lead (II), cadmium (II), copper (II) and nickel (II) by anaerobic granular biomass. *Bioresource Technology, (97), 692-700.*

Heidari, A., Younesi, H., Mehraban, Z., & Heikkinen, H. (2013). Selective adsorption of Pb (II), Cd (II), and Ni (II) ions from aqueous solution using chitosan-MAA nanoparticles. *International Journal of Biological Macromolecules, (61), 251-263.*

Ho, Y., S., Ng, J., C., Y., & McKay, G. (2011). Kinetics of pollutant sorption by biosorbents: Review. *Separation & purification Reviews, (29:2), 189-232.*

Inyang, M., I., Gao, B., Yao, Y., Xue, Y., Zimmerman, A., Mosa, A., Pullammanappallil, P., Sik, Y., & Cao, X. (2015). A review of biochar as a low-cost adsorbent for aqueous heavy metal removal. *Critical Reviews in Environmental Science and Technology, (46:4), 406-433.*

Kannan, A., & Thmbidurai, S. (2008). Removal of hexavalent chromium from aqueous solution using activated carbon derived from palmyra palm fruit seed. *Bull. Chem. Soc. Ethiop, 22(2), 183-196.*

Kooh, M., R., R., Dahri, M., K., Lim, L., B., L., Lim, L., H., & Malik, O., A. (2016). Batch adsorption studies of the removal of methyl violet 2B by soya bean waste: Isotherm, Kinetics and artificial neural network modeling. *Environ Earth Sci, (75), 783.*

Qin, B., Luo, H., Li, G., Zhang, R., Chen, S., Huo, L., & Luo, Y. (2012). Nicekl ion removal from wastewater using the microbial electrolysis cell. *Bioresourse Technology, 121,458-461.*

Laus, R., Costa, T., G., Szpoganicz, B., & Favere, V., T. (2010). Adsorption and desorption of Cu (II), Cd (II), and Pb (II) ions using chitosan crosslinked with epichlorohydrin-triphosphate as the adsorbent. Journal of Hazardous Materials, (183), 233-241.

Lopez, E., Soto, B., Arias, M., Nunez, A., Rubinos, D., & Barral, M., T. (1998). Adsorbent properties of red mud and its use for wastewater treatment. *Wat. Res., (32), 1314-1322.*

Lam, Y.F.; Lee, L.Y.; Chua, S.J.; Lim, S.S.; Gan, S. (2016) Insights into the equilibr--ium, kinetic and thermodynamics of nickel removal by environmental friendly Lansium domesticum peel biosorbent. *Ecotoxicology and Environmental Safety., (127): 61-70.*

Matouq, M., Jildeh, N., Qtaishat, M., Hindiyeh, M., & Al Syouf, M., O. (2015). The adsorption kinetics and modeling for heavy metals removal from wastewater by Moringa pods. *Journal of Environmental Chemical Engineering, (3), 775-784.*

Nadeem, R., Zafar, M., N., Afzal, A., Hanif, M., A., & Saeed, R. (2014). Potential of NaOH pretreated Mangifera indica waste biomass for the mitigation of Ni (II) and Co (II) from aqueous solution. *Journal of the Taiwan Institute of Chemical Engineers, (45), 967-972.*

Nagajyoti, P., C., Lee, K., D., & Sreekanth, T., V., M., (2010). Heavy metals, occurrence and toxicity for plants: a review. *Environ. Chem. Lett, (8), 199-*

216.

Olad, A., Ahmedi, S., & Rashidzadeh, A. (2013). Removal of Nickel from aqueous solution with polypyrrole modified clinoptilolite: Kinetic and isotherm studies. *Desalination and water Treatment, (51:37-39) 7172-7180.*

Oladipo, A., A., & Gazi, M. (2014). Enhanced removal of crystal violet by low cost alginate/acid activated bentonite composite beads:Optimization and modeling using non-linear regression technique. *Journal of Water Process Engineering, (2), 43-52.*

Oladipo, A., A., & Gazi, M. (2015). Nickel removal from aqueous solution by alginate-based composite beads: Central composite design and artificial neural network modeling. *Journal of Water Process Engineering, (8), e81-e91.*

Oladipo, A., A., & Gazi, M. (2016). Uptake of Ni^{2+} and Rhodamine B by nano-hydroxyapatite/alginate composite beads: batch and continuous-flow systems. *Toxicological & Environmental Chemistry, (98:2), 189-203.*

Popuri, S., R., Vijaya, Y., Boddu, V., M., & Abburi, K. (2009). Adsorptive removal of copper and nickel ions from water using chitosan coated PVC beads. *Bioresource Technology, (100), 194-199.*

Qin, B., Luo, H., Liu, G., Zhang, R., Chen, S., Hou, Y., & Luo, Y. (2012). Nickel ion removal from wastewater using the microbial electrolysis cell. *Bioresource*

Technology, (121), 458-461.

Regina, M. Y., Sarawathy, S., Kamal, B., Karthik, V., & Muthukmarn, k. (2015). Removal of nickel (II) ion from waste water using low cost adsorbents: A review. *Journal of Chemical and Pharmaceutical Sciences, 8(1), 0974-2115.*

Saha, S., & Sarkar, P. (2012). Arsenic remediation drinking water by synthesized nano-alumina dispersed in chitosan-grafted polyacrylamide. *Journal of Hazardous Materials, 68-78, 227-228.*

Sahoo, P., & Das, S., K. (2011). Tribology of electroless nickel coatings- A review *Materials and Design, (32), 1760-1775.*

Sheshdeh, R., K., Nikou, M., R., K., Badii, K., Limaee, N., Y., & Golkarnarenji, G. (2014). Equilibrium and kinetics studies for the adsorption of basic red 46 on nickel oxide nanoparticles-modifies diatomite in aqueous solution. *Journal of the Taiwan Institute of Chemical Engineers, (45), 1792-1802.*

Shrestha, R. M., Varga, M., Yadav, I. V. A. P., Pokharel, B. P., & Pradhananga, R. R. (2014). Removal of Ni (II) from aqueous solution by adsorption onto activated carbon prepared from lapsi (choerospondias axillaris) seed stone. *Journal of the Institute of Engineering, (9), 166-174.*

Sun, Y., Yue, Q., Gao, B., Gao, Y., Xu, X., Li, Q., & Wang, Y. (2014). Adsorption and cosorption of ciprofloxacin and Ni (II) on activated carbon-mechanism

study. *Journal of the Taiwan Institute of Chemical Engineers, (45), 681-688.*

Tan, X., Liu, Y., Zeng, G., Wang, X., Hu, X., Gu, Y., & Yang, Z. (2015). Application of biochar for the removal of pollutants from aqueous solution. *Chemosphere, (125), 70-85.*

Thakur, L., S., & Parmar, M. (2013). Adsorption of heavy metal (Cu^{2+} , Ni^{2+} and Zn^{2+}) from synthetic waste water by tea waste adsorbent. *International Journal of Chemical and Physical sciences, (2), 2391-6602.*

Tran, H., V., Tran, L., D., & Nguyen, T., N. (2010). Preparation of chitosan/magnetite composite beads and their application for removal of Pb (II) and Ni (II) from aqueous solution. *Materials Science and Engineering, C(30), 304-310.*

Villaescusa, I., Martinez, M., & Miralles, N. (2000). Heavy metal uptake from aqueous solution by cork and yohmibe bark waste. *Journal of Chemical Technology and Biotechnology, (75), 812-816.*

Wang, J., & Chen, C. (2009). Biosorbents for heavy metals removal and their future. *Biotechnology Advances, (27), 195-226.*

Xu, R., K., Xiao, S., C., Yuan, J., H., & Zhao, A., Z. (2011). Adsorption of methyl violet from aqueous solution by the biochars derived from crop residues. *Bioresource Technology,(102), 10293-10298.*

Zhang, L., Zeng, Y., & Cheng, Z. (2016). Removal of heavy metal ions using chitosan and modified chitosan: A review. *Journal of Molecular Liquids, (214), 175-191.*